

MIMO Diversity in the Presence of Double Scattering

Hyundong Shin, *Member, IEEE* and Moe Z. Win, *Fellow, IEEE*

Corresponding Author:

Hyundong Shin

Laboratory for Information and Decision Systems (LIDS)

Massachusetts Institute of Technology

Cambridge, MA 02139 USA

Tel.: (617) 253-6173

e-mail: hshin@mit.edu

This research was supported in part by the Charles Stark Draper Endowment, the Office of Naval Research Young Investigator Award N00014-03-1-0489, and the National Science Foundation under Grant ANI-0335256.

H. Shin and M. Win are with the Laboratory for Information and Decision Systems (LIDS), Massachusetts Institute of Technology, 77 Massachusetts Avenue, Cambridge, MA 02139 USA (e-mail: hshin@mit.edu, moewin@mit.edu).

Abstract

The potential benefits of multiple-antenna systems may be limited by two types of channel degradations—*rank deficiency* and *spatial fading correlation* of the channel. In this paper, we assess the effects of these degradations on the diversity performance of multiple-input multiple-output (MIMO) systems in terms of the effective fading figure (EFF), the capacity at low signal-to-noise ratio (SNR), and the symbol error probability (SEP). In particular, we consider a general family of MIMO channels known as *double-scattering* channels, which encompasses a variety of propagation environments from independent and identically distributed Rayleigh to degenerate keyhole or pinhole cases by embracing both rank-deficient and spatial correlation effects. We quantify their combined effect on the EFF and the low-SNR capacity in terms of the *correlation figures* of transmit, receive, and scatterer correlation matrices. We further show the monotonicity properties of these performance measures with respect to the strength of spatial correlation, characterized by the eigenvalue majorization relations of the correlation matrices. It is also shown that a MIMO system with n_T transmit and n_R receive antennas achieves the diversity of order $n_T n_R n_S / \max\{n_T, n_R, n_S\}$ in a double-scattering channel with n_S effective scatterers.

Index Terms

Channel capacity, diversity, double scattering, fading figure, keyhole, multiple-input multiple-output (MIMO) system, orthogonal space–time block code (OSTBC), spatial fading correlation, symbol error probability (SEP).

I. INTRODUCTION

Recent rapid advances in multiple-input multiple-output (MIMO) communication theory and growing cognizance of the tremendous performance gains achieved by MIMO techniques [1]–[9] have spurred efforts to integrate this technology into future wireless systems such as wireless local area networks (LANs) and 4G cellular systems [10]–[12]. One of the approaches to exploit diversity capability of MIMO channels is the use of orthogonal space–time block codes (OSTBCs), which have drawn considerable attention because they attain full diversity with scalar maximum-likelihood (ML) decoding [7]–[9].¹

¹However, OSTBCs with arbitrary complex constellation cannot provide the full diversity and full transmission rate simultaneously for more than two transmit antennas [8, Theorem 5.4.2] (see also [13]–[16]). A new class of quasi-orthogonal codes has been proposed in [17]–[19] with the tradeoff between the decoding complexity, transmission rate and/or diversity.

In general, the potential benefits of multiple-antenna systems may be limited by rank deficiency of the channel due to double scattering or the keyhole effect, for example, as well as spatial fading correlation due, for instance, to insufficient spacing between antenna elements [20]–[22]. All-important rank-deficient behavior of MIMO channels cannot be explained by the archetypal model based on single-scattering processes [23], [24]. To address this issue, a double-scattering MIMO model has been proposed recently in [21] wherein the channel matrix is characterized by a product of two statistically independent complex Gaussian matrices, in contrast to the common single complex Gaussian matrix characterization for wireless MIMO channels. This double-scattering model can capture both rank-deficient and spatial correlation effects of MIMO channels and encompass a variety of propagation environments, ranging from an independent and identically distributed (i.i.d.) Rayleigh case to a degenerate one-rank channel known as a keyhole or pinhole channel.

The effects of rank deficiency and spatial correlation on the capacity of MIMO channels are relatively well understood (see, e.g., [20]–[31]). From a capacity point of view, it has been known that at high signal-to-noise ratio (SNR), the spatial fading correlation reduces the diversity advantage—a parallel shift of the capacity curve over SNR in decibels (dB)—offered by multiple antennas, whereas the rank deficiency decreases the spatial multiplexing benefit—a slope of the capacity curve over SNR—of multiple-antenna channels [28].² Previously, the performance of space–time coding in the presence of spatial fading correlation has been extensively studied for the most popular Rayleigh, Rician, and Nakagami- m fading [32]–[37]. Also, the effect of rank deficiency has been investigated in [38]–[41] for a special case of the keyhole channel.

The objective of this paper is to assess the effects of double scattering on the diversity performance of MIMO systems in a communication link with n_T transmit antennas, n_R receive antennas, and n_S effective scatterers on each of the transmit and receive sides, which is referred to as a “double-scattering (n_T, n_R, n_S) -MIMO channel.” Due to the channel decoupling property, the OSTBC converts a MIMO fading channel into identical single-input single-output (SISO) Gaussian subchannels, each for a different transmitted symbol, with a path gain given by the

²Diversity in communications improves the capacity and error probability performances at *high* SNR in a different way. The benefit of diversity increases a magnitude of the slope of the error probability curve over SNR in a log-log domain, while it produces a parallel shift of the capacity curve over SNR in dB.

Frobenius norm³ of the channel matrix \mathbf{H} [35]–[39]. As a result, the maximum achievable diversity performance of MIMO systems is characterized by the statistical property of $\|\mathbf{H}\|_F$. Therefore, using the OSTBC as a pivotal MIMO diversity technique, we analyze the relevant performance measures in double-scattering (n_T, n_R, n_S) -MIMO channels, namely: i) the effective fading figure (EFF) [42]–[44], ii) the capacity in a low-SNR regime [45], [46], and iii) the symbol error probability (SEP) [47], [48]. The EFF measure is defined as a *variance-to-mean-square ratio (VMSR)* of the instantaneous SNR (see Definition 3). This quantity can be used to assess the severity of fading and the effectiveness of diversity systems on reducing signal fluctuations. The main results of this paper can be summarized as follows.

- We derive the EFF and the low-SNR capacity of double-scattering (n_T, n_R, n_S) -MIMO channels. The results show that these performance measures are completely characterized by the *correlation figures* of transmit, receive, and scatterer correlation matrices.⁴
- The EFF as a functional of the eigenvalues of correlation matrices is *monotonically increasing in a sense of Schur (MIS)*.⁵ We show that the maximum possible increase in the EFF due to double scattering is a sum of correlation figures of the transmit and receive correlation matrices, which eventuates when the scatterers tend to be fully correlated or the keyhole propagation takes place, that is, when only a single degree of freedom is available in the channel for communications.
- Regardless of the number of antennas and the presence of double scattering, the minimum received bit energy per noise level required for reliable communication, $\frac{E_b^r}{N_{0\min}}$, is equal to

$$\frac{E_b^r}{N_{0\min}} = -1.59 \text{ dB}.$$

The low-SNR capacity slope as a functional of the eigenvalues of correlation matrices is *monotonically decreasing in a sense of Schur (MDS)*. We also obtain the low-SNR capacity

³The Frobenius norm of an $m \times n$ matrix $\mathbf{A} = (A_{ij})$ is defined as

$$\|\mathbf{A}\|_F \triangleq \sqrt{\text{tr}(\mathbf{A}\mathbf{A}^\dagger)} = \left(\sum_{i=1}^m \sum_{j=1}^n |A_{ij}|^2 \right)^{1/2}$$

where $\text{tr}(\cdot)$ and \dagger denote the trace operator and the transpose conjugate of a matrix, respectively.

⁴The correlation figure is defined as a ratio of the second-order statistic of the spectra of correlation matrices to that of the fully correlated matrix (see Definition 1).

⁵See Appendix I for the notions of *Schur monotonicity* and *majorization*.

of a double-scattering MIMO channel without the constraint of orthogonal input signaling. This enables us to assess the penalty of the use of OSTBCs (for achieving full diversity with simple decoding) on spectral efficiency in the low-SNR regime or on the required bandwidth for reliable communication.

- We show that the achievable diversity is of order

$$\frac{n_T n_R n_S}{\max\{n_T, n_R, n_S\}}.$$

Hence, if the channel is “rich-enough,” that is, the number of effective scatterers is greater than or equal to the numbers of transmit and receive antennas, the full diversity order of $n_T n_R$ can be achieved even in the presence of double scattering.

- We derive exact analytical expressions for the SEP for M -ary phase shift keying (M -PSK) modulation in three cases of particular interest:
 - 1) spatially uncorrelated double scattering (includes i.i.d. and keyhole channels as special cases);
 - 2) doubly correlated double scattering (includes a spatially correlated MIMO channel where spatial correlation is present at both the transmitter and the receiver);
 - 3) multiple-input single-output (MISO) double scattering (corresponds to a pure transmit diversity system wherein a burden of diversity reception at the receive terminal is moved to the transmitter—original motivation of space–time coding [6]–[8]).

We note in passing that all the mathematical and statistical results (on the monotonicity in a sense of *Schur* and random matrices) obtained in the appendices are applicable to many other problems related to multiple-antenna communications—for example, capacity analysis of MIMO relay channels [5] and spatially correlated MIMO channels [28]–[30], and error probability analysis of multiple-antenna systems with cochannel interference [49], [50].

This paper is organized as follows. In Section II, the system model considered in the paper is presented. Section III analyzes the EFF and the low-SNR capacity (with and without the use of OSTBCs) of double-scattering (n_T, n_R, n_S) -MIMO channels. Section IV derives expressions for the SEP in the presence of double scattering. Section V concludes the paper. Apropos of our study, the notions of majorization and Schur monotonicity are briefly discussed in Appendix I. In Appendix II, we provide supplementary useful results on some statistics derived from complex

Gaussian matrices.

Notation: Throughout the paper, we shall use the following notation. \mathbb{N} , \mathbb{R} , and \mathbb{C} denote the natural numbers and the fields of real and complex numbers, respectively. The superscripts $*$, T , and \dagger stand for the complex conjugate, transpose, and transpose conjugate, respectively. \mathbf{I}_n and $\mathbf{0}_{m \times n}$ represent the $n \times n$ identity matrix and the $m \times n$ all-zero matrix, respectively. (A_{ij}) denotes the matrix with the (i, j) th entry A_{ij} and $\det_{1 \leq i, j \leq n} (A_{ij})$ is the determinant of the $n \times n$ matrix (A_{ij}) . $\text{tr}(\mathbf{A})$, $\text{etr}(\mathbf{A}) = e^{\text{tr}(\mathbf{A})}$, and $\|\mathbf{A}\|_F$ denote the trace, exponential of the trace, and Frobenius norm of the matrix \mathbf{A} , respectively. \otimes denotes the Kronecker product of matrices and $\text{vec}(\mathbf{A})$ denotes the vector formed by stacking all the columns of \mathbf{A} into a column vector. With a slight abuse of notation, a positive-semidefinite matrix \mathbf{A} is denoted by $\mathbf{A} \geq 0$ and a positive-definite matrix \mathbf{A} is denoted by $\mathbf{A} > 0$. Finally, for a Hermitian matrix $\mathbf{A} \in \mathbb{C}^{n \times n}$ with the eigenvalues $\lambda_1, \lambda_2, \dots, \lambda_n$ in any order, $\varrho(\mathbf{A})$ denotes the number of distinct eigenvalues of \mathbf{A} . Also, $\lambda_{\langle k \rangle}$ and $\ell_k(\mathbf{A})$, $k = 1, 2, \dots, \varrho(\mathbf{A})$, denote the distinct eigenvalues of \mathbf{A} in decreasing order and its multiplicity, respectively, that is, $\lambda_{\langle 1 \rangle} > \lambda_{\langle 2 \rangle} > \dots > \lambda_{\langle \varrho(\mathbf{A}) \rangle}$ and $\sum_{k=1}^{\varrho(\mathbf{A})} \ell_k(\mathbf{A}) = n$.

II. SYSTEM MODEL

We consider a MIMO wireless communication system with n_T transmit and n_R receive antennas, where the channel remains constant for N_c ($\geq n_T$) symbol periods and changes independently to a new value for each N_c -symbol coherence time. We assume that the channel is perfectly known at the receiver but unknown at the transmitter.

A. Orthogonal Space-Time Block Codes

A space-time block coded MIMO system in double-scattering channels is illustrated in Fig. 1. During an N_c -symbol interval, $N \cdot \log_2 M$ information bits are mapped to symbols x_1, x_2, \dots, x_N selected from two-dimensional signaling constellation \mathcal{S} , where $M = |\mathcal{S}|$ is the size of constellation. The symbols $\{x_k\}_{k=1}^N$ are then encoded by an OSTBC defined by an $N_c \times n_T$ transmission matrix \mathbf{G} whose entries are linear combinations of x_1, x_2, \dots, x_N and their conjugates with the property that columns of \mathbf{G} are orthogonal [8], [9]. In [13], a general construction of complex OSTBCs with the minimal delay and maximal achievable rate was presented for $n_T = N_c = 2^{N-1}$ as

$$\begin{aligned} \mathcal{G}(x_1, \dots, x_N) &= \frac{x_1}{2} (\mathbf{I}_{2^{N-1}} + \otimes^{N-1} \mathbf{J}) + \frac{x_1^*}{2} (\mathbf{I}_{2^{N-1}} - \otimes^{N-1} \mathbf{J}) \\ &\quad + \sum_{k=2}^N (\otimes^{N-k} \mathbf{I}_2) \otimes \begin{bmatrix} 0 & x_k \\ -x_k^* & 0 \end{bmatrix} \otimes (\otimes^{k-2} \mathbf{J}) \end{aligned} \quad (1)$$

where $\mathbf{J} = \begin{bmatrix} 1 & 0 \\ 0 & -1 \end{bmatrix}$ and the n th Kronecker power of a matrix \mathbf{A} is defined as

$$\otimes^n \mathbf{A} = \underbrace{\mathbf{A} \otimes \mathbf{A} \otimes \dots \otimes \mathbf{A}}_{n \text{ times}}.$$

For $2^{N-2} + k$ transmit antennas ($k = 1, 2, \dots, 2^{N-2} - 1$), the OSTBC can be obtained by simply dropping the last $2^{N-2} - k$ columns of the code (1). This construction of the OSTBC for n_T transmit antennas gives the maximal achievable rate [13, Theorem 1]

$$\mathcal{R} = \frac{\lceil \log_2 n_T \rceil + 1}{2^{\lceil \log_2 n_T \rceil}} \quad (2)$$

where $\lceil x \rceil$ denotes the smallest integer greater than or equal to x . For example, Alamouti's code $\begin{bmatrix} x_1 & x_2 \\ -x_2^* & x_1^* \end{bmatrix}$ is a one-rate OSTBC employing two transmit antennas [7] and the following code

$$\mathcal{G}_4 = \begin{bmatrix} x_1 & x_2 & x_3 & 0 \\ -x_2^* & x_1^* & 0 & -x_3 \\ -x_3^* & 0 & x_1^* & x_2 \\ 0 & x_3^* & -x_2^* & x_1 \end{bmatrix} \quad (3)$$

is a 3/4-rate OSTBC for four transmit antennas [13].

B. Signal and Channel Models

For a frequency-flat block-fading channel, the $n_R \times N_c$ received signal can be expressed in matrix notation as

$$\mathbf{Y} = \mathbf{H} \mathcal{G}^T + \mathbf{W} \quad (4)$$

where $\mathbf{H} \in \mathbb{C}^{n_R \times n_T}$ is the random channel matrix whose (i, j) th entries H_{ij} , $i = 1, 2, \dots, n_R$, $j = 1, 2, \dots, n_T$, are complex propagation coefficients between the j th transmit antenna and the i th receive antenna with $\mathbb{E}\{|H_{ij}|^2\} = 1$, and $\mathbf{W} \sim \tilde{\mathcal{N}}_{n_R, N_c}(\mathbf{0}_{n_R \times N_c}, N_0 \mathbf{I}_{n_R}, \mathbf{I}_{N_c})$ is the complex additive white Gaussian noise (AWGN) matrix (see Definition 5 and (98) in Appendix II for the

definition and distribution of complex Gaussian matrices). The total power transmitted through n_T antennas is assumed to be \mathcal{P} and hence, the average SNR per receive antenna is equal to $\bar{\gamma} \triangleq \mathcal{P}/N_0$.

For double-scattering (n_T, n_R, n_S) -MIMO channels (see Fig. 1), the channel matrix \mathbf{H} can be written as [21], [28]

$$\mathbf{H} = \frac{1}{\sqrt{n_S}} \mathbf{\Phi}_R^{1/2} \mathbf{H}_1 \mathbf{\Phi}_S^{1/2} \mathbf{H}_2 \mathbf{\Phi}_T^{1/2} \quad (5)$$

where n_S is the number of effective scatterers on each of the transmit and receive sides, \mathbf{H}_1 and \mathbf{H}_2 are statistically independent, $\mathbf{H}_1 \sim \tilde{\mathcal{N}}_{n_R, n_S}(\mathbf{0}_{n_R \times n_S}, \mathbf{I}_{n_R}, \mathbf{I}_{n_S})$, $\mathbf{H}_2 \sim \tilde{\mathcal{N}}_{n_S, n_T}(\mathbf{0}_{n_S \times n_T}, \mathbf{I}_{n_S}, \mathbf{I}_{n_T})$, and Hermitian positive-definite matrices $\mathbf{\Phi}_T$, $\mathbf{\Phi}_R$, and $\mathbf{\Phi}_S$ are $n_T \times n_T$ transmit, $n_R \times n_R$ receive, and $n_S \times n_S$ scatterer correlation matrices with all diagonal entries 1, respectively.⁶ This model can include the rank-deficient effect of MIMO channels as well as spatial fading correlation by controlling n_S and the correlation matrices $\mathbf{\Phi}_T$, $\mathbf{\Phi}_R$, and $\mathbf{\Phi}_S$. Therefore, (5) is a general family of MIMO channels spanning from the i.i.d. Rayleigh case ($n_S \rightarrow \infty$ with $\mathbf{\Phi}_T = \mathbf{I}_{n_T}$, $\mathbf{\Phi}_R = \mathbf{I}_{n_R}$, $\mathbf{\Phi}_S = \mathbf{I}_{n_S}$) to the degenerate keyhole or pinhole case ($n_S = 1$ with $\mathbf{\Phi}_T = \mathbf{I}_{n_T}$, $\mathbf{\Phi}_R = \mathbf{I}_{n_R}$) [21].

Let $\Xi_1 = \mathbf{\Phi}_R^{1/2} \mathbf{H}_1$ and $\Xi_2 = \mathbf{\Phi}_S^{1/2} \mathbf{H}_2 \mathbf{\Phi}_T^{1/2}$, then we have

$$\mathbf{H} = \frac{1}{\sqrt{n_S}} \Xi_1 \Xi_2 \quad (6)$$

where $\Xi_1 \sim \tilde{\mathcal{N}}_{n_R, n_S}(\mathbf{0}_{n_R \times n_S}, \mathbf{\Phi}_R, \mathbf{I}_{n_S})$ and $\Xi_2 \sim \tilde{\mathcal{N}}_{n_S, n_T}(\mathbf{0}_{n_S \times n_T}, \mathbf{\Phi}_S, \mathbf{\Phi}_T)$ are statistically independent complex Gaussian matrices.

C. Channel Decoupling Property of OSTBCs

With perfect channel knowledge, the receiver performs ML decoding on the OSTBC \mathcal{G} . Due to the orthogonality of columns of \mathcal{G} , space-time block decoding (signal combining) makes the ML decision metric decompose into N parts, each only a function of one and only one of

⁶In general, a correlation matrix is positive semidefinite with all diagonal entries 1. However, in this work, we restrict $\mathbf{\Phi}_T$, $\mathbf{\Phi}_R$, and $\mathbf{\Phi}_S$ to positive-definite matrices. This implies that the rank of \mathbf{H} is equal to $\min\{n_T, n_R, n_S\}$ with probability one. Therefore, rank deficiency can be distinguished from the spatial correlation effect and may occur only due to double scattering with n_S less than $\min\{n_T, n_R\}$. This also enables us to discriminate a one-rank *fully* correlated scenario from a degenerate keyhole MIMO channel [27].

x_1, x_2, \dots, x_N [8], [9]. Therefore, as shown in Fig. 1, orthogonal space–time block encoding and decoding convert a MIMO fading channel into N equivalent SISO Gaussian subchannels, each for a different symbol, with a path gain given by the Frobenius norm of the channel matrix [35]–[39]. More specifically, the input-output relation of the induced SISO subchannel for x_k , $k = 1, 2, \dots, N$, can be written as [38], [39]

$$\tilde{y}_k = \|\mathbf{H}\|_{\text{F}} x_k + \tilde{w}_k \quad (7)$$

and the ML receiver chooses \hat{x}_k for x_k if and only if

$$\hat{x}_k = \arg \min_{x \in \mathcal{S}} \left| \tilde{y}_k - \|\mathbf{H}\|_{\text{F}} x \right|^2 \quad (8)$$

where $\tilde{w}_k \sim \mathcal{CN}(0, N_0)$ is the Gaussian noise after signal combining.⁷ Consequently, the performance of OSTBCs is completely characterized by the statistical behavior of $\|\mathbf{H}\|_{\text{F}}$ and the instantaneous received SNR for each of the SISO subchannels, denoted by γ_{STBC} , is given by [38], [39]

$$\begin{aligned} \gamma_{\text{STBC}} &= \|\mathbf{H}\|_{\text{F}}^2 \frac{\mathbb{E}\{|x_k|^2\}}{N_0} \\ &= \frac{\bar{\gamma} \|\mathbf{H}\|_{\text{F}}^2}{n_{\text{T}} \mathcal{R}}. \end{aligned} \quad (9)$$

III. EFFECTIVE FADING FIGURE AND LOW-SNR CAPACITY

In this section, we access the combined effect of rank deficiency and spatial correlation on the performance of OSTBCs in terms of the EFF and the capacity in a low-SNR regime. It will be apparent that these performance measures are completely characterized by the *kurtosis* of $\|\mathbf{H}\|_{\text{F}}$.

A. Kurtosis of $\|\mathbf{H}\|_{\text{F}}$

The kurtosis measures the peakedness or flatness of a distribution [51]. By definition, the kurtosis of $\|\mathbf{H}\|_{\text{F}}$, denoted by $\kappa(\|\mathbf{H}\|_{\text{F}})$, is given by

$$\begin{aligned} \kappa(\|\mathbf{H}\|_{\text{F}}) &\triangleq \frac{\mathbb{E}\{[\|\mathbf{H}\|_{\text{F}} - \mathbb{E}\{\|\mathbf{H}\|_{\text{F}}\}]^4\}}{(\mathbb{E}\{[\|\mathbf{H}\|_{\text{F}} - \mathbb{E}\{\|\mathbf{H}\|_{\text{F}}\}]^2\})^2} \\ &= \frac{\mathbb{E}\{\|\mathbf{H}\|_{\text{F}}^4\}}{(\mathbb{E}\{\|\mathbf{H}\|_{\text{F}}^2\})^2} \end{aligned} \quad (10)$$

⁷ $\mathcal{CN}(\mu, \sigma^2)$ denotes a circularly symmetric complex Gaussian distribution with mean μ and variance σ^2 .

where the second equality follows from the fact that the kurtosis is invariant with respect to translations of a random variable. It has been shown that this normalized form of the fourth statistic plays a key role in the low-SNR behavior of the spectral efficiency of fading channels [45], [52]. To proceed with deriving $\kappa(\|\mathbf{H}\|_F)$ for double-scattering (n_T, n_R, n_S) -MIMO channels, we first define the following scalar quantity related to a correlation matrix.

Definition 1 (Correlation Figure): For an arbitrary $n \times n$ correlation matrix Φ , the *correlation figure* of Φ is defined by

$$\zeta(\Phi) \triangleq \frac{\text{tr}(\Phi^2)}{\text{tr}(\mathbf{1}_n^2)} = \frac{1}{n^2} \text{tr}(\Phi^2) \quad (11)$$

where $\mathbf{1}_n$ denotes the $n \times n$ all-one matrix.

Note that $\frac{1}{n} \leq \zeta(\Phi) \leq 1$, where the lower and upper bounds correspond to uncorrelated and fully correlated cases, respectively.⁸ The following theorem shows that $\kappa(\|\mathbf{H}\|_F)$ depends exclusively on the spectra of spatial correlation matrices and is quantified solely by their correlation figures.

Theorem 1: For double-scattering (n_T, n_R, n_S) -MIMO channels, the kurtosis of $\|\mathbf{H}\|_F$ is

$$\kappa(\|\mathbf{H}\|_F) = \zeta(\Phi_T) \zeta(\Phi_R) + \zeta(\Phi_T) \zeta(\Phi_S) + \zeta(\Phi_R) \zeta(\Phi_S) + 1. \quad (12)$$

Proof: Using Theorem 7 in Appendix II, we get

$$\begin{aligned} \mathbb{E}\{\|\mathbf{H}\|_F^4\} &= \mathbb{E}_{\Xi_1, \Xi_2} \left\{ \text{tr}^2 \left(\frac{1}{n_S} \Xi_1 \Xi_2 \Xi_2^\dagger \Xi_1^\dagger \right) \right\} \\ &= \left(\frac{n_R}{n_S} \right)^2 \text{tr}(\Phi_T^2) \text{tr}(\Phi_S^2) + \text{tr}(\Phi_T^2) \text{tr}(\Phi_R^2) + \left(\frac{n_T}{n_S} \right)^2 \text{tr}(\Phi_R^2) \text{tr}(\Phi_S^2) + (n_T n_R)^2. \end{aligned} \quad (13)$$

Combining (10), (11), and (13), together with the fact that $\mathbb{E}\{\|\mathbf{H}\|_F^2\} = n_T n_R$, yields the desired result. \square

⁸Similar to (11), the *correlation number* was defined as $\frac{1}{n} \text{tr}(\Phi^2)$ [46]. While the correlation figure and number are the second-order statistics of the spectra of a correlation matrix, normalized by those of fully correlated and uncorrelated matrices, respectively, the correlation figure is bounded by $0 \leq \zeta(\Phi) \leq 1$ for any correlation structure, as $n \rightarrow \infty$.

Example 1 (Spatially Uncorrelated Double Scattering): In the absence of spatial fading correlation ($\Phi_T = I_{n_T}$, $\Phi_R = I_{n_R}$, $\Phi_S = I_{n_S}$), we have

$$\kappa(\|H\|_F) = \frac{1}{n_T n_R} + \frac{1}{n_T n_S} + \frac{1}{n_R n_S} + 1. \quad (14)$$

The i.i.d. and keyhole MIMO channels are two extreme cases of spatially uncorrelated double scattering (i.e., $n_S = \infty$ and $n_S = 1$, respectively). As compared with the i.i.d. case, the keyhole increases the kurtosis of the fading distribution in SISO subchannels by twice the reciprocal of the harmonic mean between the numbers of transmit and receive antennas, that is, $\frac{1}{n_T} + \frac{1}{n_R}$.

Next, we show that $\kappa(\|H\|_F)$ as a functional of the eigenvalues of Φ_T , Φ_R , and Φ_S is MIS. To do this, we first provide the following definition to characterize a spatial correlation environment of double-scattering MIMO channels.

Definition 2: Given n_T , n_R , and n_S , a spatial correlation environment of double-scattering channels is denoted by $\bar{\Phi} = (\Phi_T, \Phi_R, \Phi_S)$. For two different spatial correlation environments $\bar{\Phi}_1 = (\Phi_T, \Phi_R, \Phi_S)$ and $\bar{\Phi}_2 = (\Phi_T, \Phi_R, \Phi_S)$, we denote $\bar{\Phi}_1 \preceq \bar{\Phi}_2$ and simply say that $\bar{\Phi}_1$ is *majorized* by $\bar{\Phi}_2$ if $\Phi_T \preceq \Phi_T$, $\Phi_R \preceq \Phi_R$, and $\Phi_S \preceq \Phi_S$.

Corollary 1: The kurtosis of $\|H\|_F$, as a functional of the eigenvalues of correlation matrices, is a MIS (or isotone) function, that is, if $\bar{\Phi}_1 \preceq \bar{\Phi}_2$, then

$$\kappa(\|H\|_F; \bar{\Phi}_1) \leq \kappa(\|H\|_F; \bar{\Phi}_2). \quad (15)$$

Proof: It follows immediately from Theorem 1, Corollary 4 in Appendix I, and the fact that the correlation figure is nonnegative. \square

Corollary 1 implies that the less spatially correlated fading results in the less peaky fading distribution of each SISO subchannel.

B. Effective Fading Figure

One of the goals of diversity systems is to reduce the signal fluctuation due to the stochastic nature of multipath fading. Therefore, it is of interest to characterize the variation of the instantaneous SNR at the output where the amount of signal fluctuations is measured. The following measure can be used to assess the severity of fading and the effectiveness of diversity systems on reducing signal fluctuations.

Definition 3 (Effective Fading Figure): For the instantaneous SNR γ at the output of interest in a communication system subject to fading, the effective fading figure (EFF) in dB for the output SNR γ is defined as the VMSR of γ , i.e.,

$$\text{EFF}_\gamma \text{ (dB)} \triangleq 10 \log_{10} \left\{ \frac{\text{Var} \{ \gamma \}}{(\mathbb{E} \{ \gamma \})^2} \right\}. \quad (16)$$

It should be noted that the EFF is akin to the notions of the normalized standard deviation (NSD) of the instantaneous combiner output SNR [42]–[44] and the amount of fading (AF) [53]. The AF, as defined in [53, eq. (2)], is purely to characterize the amount of random fluctuations in the channel itself and conveys no information about diversity systems. In contrast, the NSD is a measure of the signal fluctuations at the diversity combiner output, enabling us to compare the effectiveness of diversity combining techniques such as maximal-ratio combining (MRC), equal-gain combining (EGC), selection combining (SC), and hybrid selection/maximal-ratio combining (H-S/MRC). If the signal fluctuation is measured at each branch output, the EFF is synonymous with the AF. In contrast, when the signal fluctuation is measured at the diversity combiner output, the EFF is equal to the square of the NSD of the instantaneous SNR at the combiner output.

Since the use of OSTBCs is to mitigate the detrimental effect of fading by means of diversity, the efficiency of OSTBCs on reducing the severity of fading can be assessed by

$$\begin{aligned} \text{EFF}_{\text{STBC}} \text{ (dB)} &\triangleq 10 \log_{10} \left\{ \frac{\text{Var} \{ \gamma_{\text{STBC}} \}}{(\mathbb{E} \{ \gamma_{\text{STBC}} \})^2} \right\} \\ &= 10 \log_{10} \{ \kappa (\| \mathbf{H} \|_F) - 1 \}. \end{aligned} \quad (17)$$

Note that the minimum EFF is equal to $-\infty$ dB if there is no random fluctuation in the received signal. Also, the EFF is equal to 0 dB for Rayleigh fading without diversity and hence, $\text{EFF}_{\text{STBC}} > 0$ dB means that the variation of the instantaneous SNR in each SISO subchannel is more severe than that in Rayleigh fading.

From Theorem 1 and (17), it is straightforward to see that the EFF_{STBC} in double-scattering (n_T, n_R, n_S) -MIMO channels is given by

$$\text{EFF}_{\text{STBC}} \text{ (dB)} = 10 \log_{10} \{ \zeta(\Phi_T) \zeta(\Phi_R) + \zeta(\Phi_T) \zeta(\Phi_S) + \zeta(\Phi_R) \zeta(\Phi_S) \} \quad (18)$$

from which we can make the following observations on the EFF_{STBC} .

- The EFF_{STBC} as a functional of the eigenvalues of correlation matrices is MIS, that is,

$$\text{EFF}_{\text{STBC}}(\bar{\Phi}_1) \leq \text{EFF}_{\text{STBC}}(\bar{\Phi}_2) \quad (19)$$

whenever $\bar{\Phi}_1 \preceq \bar{\Phi}_2$. This reveals that the less spatially correlated fading results in the less severe random fluctuations in equivalent SISO subchannels induced by OSTBCs.

- The EFF_{STBC} is symmetric with respect to n_T , n_R , n_S , and the spatial correlation properties on the transmitter, receiver, and scatterers.
- For fixed numbers of transmit and receive antennas, the EFF_{STBC} is bounded by

$$-10 \log_{10}(n_T n_R) \text{ dB} \leq \text{EFF}_{\text{STBC}} < 4.77 \text{ dB}. \quad (20)$$

The lower bound of the EFF_{STBC} is the same as the EFF at the MRC output of order $n_T n_R$ in Rayleigh fading, which is achieved when the spatial fading is uncorrelated in the absence of double scattering. The upper bound of the EFF_{STBC} is equal to three times as large as the EFF of Rayleigh fading, which corresponds to a fading situation more severe than a one-sided Gaussian channel (without diversity) whose EFF is equal to 3 dB.

- In the absence of double scattering, $\zeta(\Phi_S)$ is equal to zero and thus, the double scattering together with spatial correlation causes the EFF_{STBC} to increase by the amount of $\zeta(\Phi_T) \zeta(\Phi_S) + \zeta(\Phi_R) \zeta(\Phi_S)$. In particular, the maximum increase in the EFF_{STBC} is a sum of correlation figures of the transmit and receive correlation matrices, that is, $\zeta(\Phi_T) + \zeta(\Phi_R)$, which eventuates when Φ_S goes to be fully correlated or when the keyhole effect takes place.
- In the presence of spatially uncorrelated double scattering, we have

$$\text{EFF}_{\text{STBC}} \text{ (dB)} = 10 \log_{10} \left\{ \frac{1}{n_T n_R} + \underbrace{\frac{1}{n_S} \left(\frac{1}{n_T} + \frac{1}{n_R} \right)}_{\text{increase in } \text{EFF}_{\text{STBC}} \text{ due to spatially uncorrelated double scattering}} \right\}. \quad (21)$$

The maximum increase in the EFF_{STBC} due to spatially uncorrelated double scattering is equal to $\frac{1}{n_T} + \frac{1}{n_R}$, which is incurred by the keyhole effect, in agreement with [39, eq. (18)].

C. Low-SNR Capacity

Recent information-theoretic studies show that the first-order analysis of the capacity versus the SNR fails to reveal the impact of the channel and that second-order analysis is required to

assess the wideband or low-SNR performance of communication systems [45], [46]. In particular, it was demonstrated that the tradeoff between the capacity in bits/s/Hz and energy per bit required for reliable communication is the key measure of channel capacity in a low-SNR regime.

As in [45] and [46], we are now interested in the behavior of capacity in the low-SNR regime. In this regime, the capacity can be characterized by two parameters, namely, i) $\frac{E_b}{N_0 \min}$, the *minimum bit energy per noise level* required to reliably communicate at any positive data rate (where E_b denotes the total transmitted energy per bit), and ii) S_0 , the *low-SNR slope* (bits/s/Hz per 3 dB) of the capacity at the point $\frac{E_b}{N_0 \min}$. These two quantities determine the first-order behavior of the capacity in bits/s/Hz versus $\frac{E_b}{N_0}$ as follows [45], [46]:

$$\begin{aligned} C\left(\frac{E_b}{N_0}\right) &= C(\bar{\gamma}) \\ &= S_0 \log_2 \left(\frac{\frac{E_b}{N_0}}{\frac{E_b}{N_0 \min}} \right) + o(\bar{\gamma}) \quad \text{as } \bar{\gamma} \rightarrow 0 \end{aligned} \quad (22)$$

where $C(\bar{\gamma})$ is the channel capacity in bits/s/Hz as a function of the SNR $\bar{\gamma}$ that is the solution to

$$\frac{E_b}{N_0} C(\bar{\gamma}) = \bar{\gamma}. \quad (23)$$

As shown in [45], $\frac{E_b}{N_0 \min}$ and S_0 satisfy

$$\frac{E_b}{N_0 \min} = \lim_{\bar{\gamma} \rightarrow 0} \frac{\bar{\gamma}}{C(\bar{\gamma})} = \frac{1}{\dot{C}(0)} \quad (24)$$

and

$$\begin{aligned} S_0 &= \lim_{\frac{E_b}{N_0} \rightarrow \frac{E_b}{N_0 \min}} \frac{C\left(\frac{E_b}{N_0}\right)}{\log_2\left(\frac{E_b/N_0}{E_b/N_0 \min}\right)} \\ &= \frac{-2[\dot{C}(0)]^2}{\ddot{C}(0)} \log_e 2 \quad \text{bits/s/Hz per 3 dB} \end{aligned} \quad (25)$$

where $\dot{C}(0)$ and $\ddot{C}(0)$ are the first and second derivatives of $C(\bar{\gamma})$ at $\bar{\gamma} = 0$. Note that the first-order approximation to $C(\frac{E_b}{N_0})$ reflects the second-order behavior of $C(\bar{\gamma})$ and the first-order derivative of $C(\bar{\gamma})$ can exhibit no other than the quantity $\frac{E_b}{N_0 \min}$ in understanding the behavior of capacity in the low-SNR regime [46].

1) *General Input Signaling:* Before proceeding to study the low-SNR capacity achieved by OSTBCs, we first deal with the more general case of input signaling, assuming that the fading process is ergodic and coding is across many independent fading blocks without a delay constraint.

Theorem 2: Consider a general double-scattering (n_T, n_R, n_S) -MIMO channel

$$\mathbf{Y} = \mathbf{H}\mathbf{X} + \mathbf{W} \quad (26)$$

where the channel matrix \mathbf{H} is given by (5) at each N_c -symbol coherence interval and the input signal $\mathbf{X} \in \mathbb{C}^{n_T \times N_c}$ is subject to the power constraint $\mathbb{E} \{\|\mathbf{X}\|_F^2\} = N_c \mathcal{P}$. Suppose that the receiver knows the realization of \mathbf{H} , but the transmitter has no channel knowledge. Then, the minimum required $\frac{E_b}{N_0}$ for reliable communication is

$$\frac{E_b}{N_{0\min}} = \frac{\log_e 2}{n_R} \quad (27)$$

and the low-SNR slope of the capacity is

$$S_0 = \frac{2}{\zeta(\Phi_T) + \zeta(\Phi_R) + \zeta(\Phi_S) + \zeta(\Phi_T)\zeta(\Phi_R)\zeta(\Phi_S)}. \quad (28)$$

Proof: In this case, the ergodic capacity (or Shannon-sense mean capacity) is given by the well-known expression [2]–[4]

$$C(\bar{\gamma}) = \mathbb{E} \left\{ \log_2 \det \left(\mathbf{I}_{n_R} + \frac{\bar{\gamma}}{n_T} \mathbf{H}\mathbf{H}^\dagger \right) \right\} \quad \text{bits/s/Hz} \quad (29)$$

which is achieved by the complex Gaussian input $\mathbf{X} \sim \tilde{\mathcal{N}}_{n_T, N_c}(\mathbf{0}_{n_T \times N_c}, \frac{\mathcal{P}}{n_T} \mathbf{I}_{n_T}, \mathbf{I}_{N_c})$.

From (24) and (25), we get

$$\frac{E_b}{N_{0\min}} = \frac{n_T \log_e 2}{\mathbb{E} \{\|\mathbf{H}\|_F^2\}} = \frac{\log_e 2}{n_R} \quad (30)$$

and

$$\begin{aligned} S_0 &= \frac{2 (\mathbb{E} \{\|\mathbf{H}\|_F^2\})^2}{\mathbb{E} \left\{ \text{tr} \left[(\mathbf{H}\mathbf{H}^\dagger)^2 \right] \right\}} \\ &= \frac{2 (n_T n_R n_S)^2}{\mathbb{E}_{\Xi_1, \Xi_2} \left\{ \text{tr} \left[\left(\Xi_1 \Xi_2 \Xi_2^\dagger \Xi_1^\dagger \right)^2 \right] \right\}}. \end{aligned} \quad (31)$$

Using Definition 1 and Theorem 7 in Appendix II, (31) can be expressed in terms of the correlation figures of Φ_T , Φ_R , and Φ_S as in (28). \square

Recall that the low-SNR slope S_0 is reciprocally proportional to the required bandwidth B to sustain a given data rate R (bits/s) with power \mathcal{P} [45], [46]:

$$B \approx \frac{R}{S_0} \frac{3 \text{ dB}}{\left. \frac{\mathcal{P}}{RN_0} \right|_{\text{dB}} - \left. \frac{E_b}{N_0} \right|_{\text{min}}}. \quad (32)$$

Hence, for fixed data rate and power, the required bandwidth B relative to the bandwidth B_{iid} required in the absence of double scattering and spatial correlation is

$$\frac{B}{B_{\text{iid}}} = \frac{1}{S_0} \cdot \underbrace{\frac{2n_T n_R}{n_T + n_R}}_{S_{0,\text{iid}}} \quad (33)$$

which represents a expansion factor of the bandwidth required for reliable communication, due to double scattering and spatial correlation. In (33), $S_{0,\text{iid}}$ is the low-SNR slope in the absence of double scattering and spatial correlation, obtained by letting $\zeta(\Phi_T) = \frac{1}{n_T}$, $\zeta(\Phi_R) = \frac{1}{n_R}$, and $\zeta(\Phi_S) = 0$ in (28).

From Theorem 2 and (33), we can make the following observations.

- The $\frac{E_b}{N_{0\text{min}}}$ is inversely proportional to n_R , whereas the double scattering and spatial fading correlation as well as the numbers of transmit antennas and effective scatterers do not affect this measure. Moreover, regardless of the number of antennas and propagation conditions, the minimum received bit energy per noise level required for reliable communication, $\frac{E_b^r}{N_{0\text{min}}}$, is equal to

$$\frac{E_b^r}{N_{0\text{min}}} = n_R \cdot \frac{E_b}{N_{0\text{min}}} = -1.59 \text{ dB} \quad (34)$$

which is a fundamental feature of the channels where the additive noise is Gaussian [45, Theorem 1].

- The low-SNR slope S_0 as a functional of the eigenvalues of correlation matrices is MDS, that is, if $\bar{\Phi}_1 \preceq \bar{\Phi}_2$, then

$$S_0(\bar{\Phi}_1) \geq S_0(\bar{\Phi}_2) \quad (35)$$

which follows from (28), Corollary 4, and the non-negativeness of correlation figures. This MDS property reveals that the low-SNR slope decreases with the amount of spatial correlation in contrast to the high-SNR capacity slope, $\min\{n_T, n_R, n_S\}$, which is invariant with respect to spatial correlation [28].

- For fixed numbers of transmit and receive antennas, the low-SNR slope is greater than 0.5 and less than or equal to the harmonic mean of n_T and n_R , that is,

$$0.5 < S_0 \leq \frac{2n_T n_R}{n_T + n_R} \quad (36)$$

where the lowest slope is achieved if the correlation matrices tend to be fully correlated and the highest slope is achieved in the absence of double scattering and spatial correlation. Also, the bandwidth expansion factor for fixed numbers of antennas, data rate, and power is bounded by

$$1 \leq \frac{B}{B_{\text{iid}}} < \frac{4n_T n_R}{n_T + n_R}. \quad (37)$$

- In the absence of spatial correlation, the low-SNR slope is given by

$$S_0 = \frac{2n_T n_R}{n_T + n_R} \cdot \underbrace{\left(1 + \frac{1}{n_S} \cdot \frac{n_T n_R + 1}{n_T + n_R}\right)^{-1}}_{\text{bandwidth expansion due to spatially uncorrelated double scattering}}. \quad (38)$$

The maximum bandwidth expansion due to spatially uncorrelated double scattering is equal to $1 + \frac{n_T n_R + 1}{n_T + n_R}$, which is incurred by the keyhole effect.

Example 2 (Dual-Antenna System): Consider $n_T = n_R = 2$. In the presence of spatially uncorrelated double scattering, the low-SNR slope for general double-scattering $(2, 2, n_S)$ -MIMO channels is

$$S_0 = 2 \cdot \left(1 + \frac{1}{n_S} \cdot \frac{5}{4}\right)^{-1} \text{ bits/s/Hz per 3 dB}, \quad (39)$$

which is bounded by $8/9 \leq S_0 \leq 2$. The lowest and highest slopes are achieved when $n_S = 1$ (keyhole) and $n_S = \infty$ (i.i.d.), respectively. Also, the maximum bandwidth expansion $\frac{B}{B_{\text{iid}}}$ due to the keyhole effect is equal to $9/4$. Thus, if the keyhole propagation takes place, the required

bandwidth for reliable communication (with fixed data rate and power) is *more than twice* as large as for i.i.d. channels.

2) *OSTBC Input Signaling*: We now turn attention to the low-SNR behavior of the capacity for double-scattering (n_T, n_R, n_S) -MIMO channels employing OSTBCs.

Theorem 3: Consider a double-scattering (n_T, n_R, n_S) -MIMO channel

$$\mathbf{Y} = \mathbf{H}\mathbf{G}^T + \mathbf{W}$$

where the channel matrix \mathbf{H} is given by (5) at each N_c -symbol coherence interval and the OSTBC \mathbf{G} is subject to the power constraint $\mathbb{E}\{\|\mathbf{G}\|_F^2\} = N_c\mathcal{P}$. Then, the OSTBC achieves the minimum required $\frac{E_b}{N_0 \min}$ same as that without the orthogonal signaling constraint

$$\frac{E_b}{N_0 \min}^{\text{STBC}} = \frac{\log_e 2}{n_R} \quad (40)$$

and the low-SNR slope of the capacity

$$S_0^{\text{STBC}} = \frac{2\mathcal{R}}{\zeta(\Phi_T)\zeta(\Phi_R) + \zeta(\Phi_T)\zeta(\Phi_S) + \zeta(\Phi_R)\zeta(\Phi_S) + 1}. \quad (41)$$

Proof: Due to the channel decoupling property of OSTBCs, the Shannon capacity of OSTBC MIMO channels can be written as

$$C_{\text{STBC}}(\bar{\gamma}) = \mathcal{R} \cdot \mathbb{E} \left\{ \log_2 \left(1 + \frac{\bar{\gamma} \|\mathbf{H}\|_F^2}{n_T \mathcal{R}} \right) \right\} \quad \text{bits/s/Hz} \quad (42)$$

which is achieved by complex Gaussian inputs $x_k \sim \mathcal{CN}(0, \frac{\mathcal{P}}{n_T \mathcal{R}})$. From the first and second derivatives of (42) at $\bar{\gamma} = 0$, it is easy to show (40) and

$$S_0^{\text{STBC}} = \frac{2\mathcal{R}}{\kappa(\|\mathbf{H}\|_F)} \quad (43)$$

from which and Theorem 1, (41) follows readily. \square

We remark that as compared with the general case, the use of OSTBCs does not increase the minimum required $\frac{E_b}{N_0}$ for reliable communication in MIMO channels and S_0^{STBC} has the same MDS property as for S_0 in III-C.1. In contrast, we see from (42) that the high-SNR slope of the

capacity is equal to \mathcal{R} , which does not depend on spatial correlation. Also, for fixed data rate and power, the required bandwidth for OSTBC MIMO channels is expanded by a factor

$$\frac{B^{\text{STBC}}}{B_{\text{iid}}^{\text{STBC}}} = \kappa(\|\mathbf{H}\|_{\text{F}}) \cdot \frac{n_{\text{T}}n_{\text{R}}}{n_{\text{T}}n_{\text{R}} + 1} \quad (44)$$

due to double scattering and spatial correlation. In addition, we can observe the following in parallel to III-C.1.

- For fixed numbers of antennas, the low-SNR slope and bandwidth expansion factor are bounded respectively by

$$0.5 \mathcal{R} < S_0^{\text{STBC}} \leq \mathcal{R} \cdot \frac{2n_{\text{T}}n_{\text{R}}}{n_{\text{T}}n_{\text{R}} + 1} \quad (45)$$

$$1 \leq \frac{B^{\text{STBC}}}{B_{\text{iid}}^{\text{STBC}}} < \frac{4n_{\text{T}}n_{\text{R}}}{n_{\text{T}}n_{\text{R}} + 1}. \quad (46)$$

- In the absence of spatial correlation, the low-SNR slope is given by

$$S_0^{\text{STBC}} = \mathcal{R} \cdot \frac{2n_{\text{T}}n_{\text{R}}}{n_{\text{T}}n_{\text{R}} + 1} \cdot \underbrace{\left(1 + \frac{1}{n_{\text{S}}} \cdot \frac{n_{\text{T}} + n_{\text{R}}}{n_{\text{T}}n_{\text{R}} + 1}\right)^{-1}}_{\text{bandwidth expansion due to spatially uncorrelated double scattering}}. \quad (47)$$

The maximum bandwidth expansion $\frac{B^{\text{STBC}}}{B_{\text{iid}}^{\text{STBC}}}$ due to spatially uncorrelated double scattering is equal to $1 + \frac{n_{\text{T}}+n_{\text{R}}}{n_{\text{T}}n_{\text{R}}+1}$, which is incurred by the keyhole effect.

Example 3 (Alamouti's Code): Consider $n_{\text{T}} = n_{\text{R}} = 2$. In the presence of spatially uncorrelated double scattering, the low-SNR slope for Alamouti's code with two receive antennas is

$$S_0^{\text{STBC}} = \frac{8}{5} \cdot \left(1 + \frac{1}{n_{\text{S}}} \cdot \frac{4}{5}\right)^{-1} \text{ bits/s/Hz per 3 dB} \quad (48)$$

which is bounded by $8/9 \leq S_0^{\text{STBC}} \leq 8/5$. The maximum bandwidth expansion $\frac{B^{\text{STBC}}}{B_{\text{iid}}^{\text{STBC}}}$ due to the keyhole effect is equal to $9/5$ (which is less than the corresponding value for the general input signaling in Example 2). Thus, the required bandwidth for reliable communication in the keyhole channel is *almost twice* as large as that in the i.i.d. channel.

Finally, we give the following result that provides insights into the effect of the use of OSTBCs on the required bandwidth for reliable communication.

Corollary 2: For fixed data rate and power, the required bandwidth for reliable communication is expanded due to the OSTBC signaling constraint by a factor

$$\frac{B^{\text{STBC}}}{B} = \frac{1}{2\mathcal{R}} \kappa(\|\mathbf{H}\|_{\text{F}}) S_0 \quad (49)$$

in double-scattering $(n_{\text{T}}, n_{\text{R}}, n_{\text{S}})$ -MIMO channels. This bandwidth expansion factor as a functional of the eigenvalues of correlation matrices is MDS, that is, if $\bar{\Phi}_1 \preceq \bar{\Phi}_2$, then

$$\frac{B^{\text{STBC}}}{B}(\bar{\Phi}_1) \geq \frac{B^{\text{STBC}}}{B}(\bar{\Phi}_2). \quad (50)$$

Thus, the penalty of the OSTBC signaling constraint on the required bandwidth for fixed numbers of antennas, data rate, and power decreases with the strength of spatial correlation.

Proof: From Theorems 2 and 3 together with (32), it is straightforward to obtain (49). To prove monotonicity (50), we first show that the expansion factor $\frac{B^{\text{STBC}}}{B}$ as a functional of the eigenvalues of Φ_{T} is MDS.

Let $\lambda_1, \lambda_2, \dots, \lambda_{n_{\text{T}}}$ be the eigenvalues of Φ_{T} . Then, since $\frac{B^{\text{STBC}}}{B}$ is symmetric in $\lambda_1, \lambda_2, \dots, \lambda_{n_{\text{T}}}$, it is sufficient to show the Schur's condition (see Theorem 6 in Appendix I):

$$(\lambda_1 - \lambda_2) \left[\frac{\partial}{\partial \lambda_1} \frac{B^{\text{STBC}}}{B}(\bar{\Phi}) - \frac{\partial}{\partial \lambda_2} \frac{B^{\text{STBC}}}{B}(\bar{\Phi}) \right] \leq 0. \quad (51)$$

It can be shown by differentiating (49) that

$$\frac{\partial}{\partial \lambda_i} \frac{B^{\text{STBC}}}{B}(\bar{\Phi}) = \frac{S_0^2}{4\mathcal{R}} \cdot [\zeta^2(\Phi_{\text{R}}) + \zeta^2(\Phi_{\text{S}}) - \zeta^2(\Phi_{\text{R}})\zeta^2(\Phi_{\text{S}}) - 1] \cdot \frac{\partial \zeta(\Phi_{\text{T}})}{\partial \lambda_i}, \quad (52)$$

therefore

$$\begin{aligned} & \frac{\partial}{\partial \lambda_1} \frac{B^{\text{STBC}}}{B}(\bar{\Phi}) - \frac{\partial}{\partial \lambda_2} \frac{B^{\text{STBC}}}{B}(\bar{\Phi}) \\ &= \frac{S_0^2}{4\mathcal{R}} \cdot (\zeta^2(\Phi_{\text{R}}) - 1)(1 - \zeta^2(\Phi_{\text{S}})) \cdot \left[\frac{\partial \zeta(\Phi_{\text{T}})}{\partial \lambda_1} - \frac{\partial \zeta(\Phi_{\text{T}})}{\partial \lambda_2} \right]. \end{aligned} \quad (53)$$

Since the correlation figure is MIS and less than or equal to 1, we have

$$(\zeta^2(\Phi_R) - 1)(1 - \zeta^2(\Phi_S)) \leq 0 \quad (54)$$

$$(\lambda_1 - \lambda_2) \left[\frac{\partial \zeta(\Phi_T)}{\partial \lambda_1} - \frac{\partial \zeta(\Phi_T)}{\partial \lambda_2} \right] \geq 0, \quad (55)$$

which, together with the fact that $S_0 \geq 0$, show that Schur's condition holds.

Since $\frac{B^{\text{STBC}}}{B}$ is symmetric in the correlation figures of Φ_T , Φ_R , and Φ_S , the similar argument shows the same monotonicity property for Φ_R and Φ_S . Hence, we complete the proof. \square

Fig. 2 shows the variation of the bandwidth expansion $\frac{B^{\mathcal{G}_4}}{B}$ (due to the use of OSTBC \mathcal{G}_4) with a correlation coefficient ρ for $n_T = n_R = 4$ and various numbers of the effective scatterers. In this figure, spatial correlation at the transmitter, the receiver, and the scatterers follows exponential correlation, defined in (83), $\Phi_T = \Phi_R = \Phi_4^{(e)}(\rho)$ and $\Phi_S = \Phi_{n_S}^{(e)}(\rho)$. From Fig. 2, we can observe that the bandwidth expansion $\frac{B^{\mathcal{G}_4}}{B}$ is bounded by $4/3 \leq \frac{B^{\mathcal{G}_4}}{B} \leq 5/3$ and decreases as ρ increases. The minimum and maximum values of $\frac{B^{\mathcal{G}_4}}{B}$ correspond to the keyhole and i.i.d. channels, respectively. In particular, for the keyhole channel, (49) becomes $1/\mathcal{R}$ and hence, the rate \mathcal{R} of the OSTBC solely reflects the bandwidth expansion due to the use of the OSTBC, irrespective of spatial correlation. Also, $\frac{B^{\mathcal{G}_4}}{B}$ increases with n_S , because the OSTBC cannot utilize the multiplexing ability of MIMO channels.

In Fig. 3, the capacity (bits/s/Hz) versus $\frac{E_b^r}{N_0 \min}$ and its low-SNR approximation are depicted with and without the signaling constraint of the OSTBC \mathcal{G}_4 in double-scattering $(4, 4, 20)$ -MIMO channels with exponential correlation $\Phi_T = \Phi_R = \Phi_4^{(e)}(0.5)$ and $\Phi_S = \Phi_{20}^{(e)}(0.5)$. For the OSTBC \mathcal{G}_4 , the low-SNR approximation is remarkably accurate for a fairly wide range of $\frac{E_b^r}{N_0 \min}$, whereas there exists some discrepancy between the Monte Carlo simulation and the first-order approximation for the general input signaling—approximately 11% difference at $\frac{E_b^r}{N_0 \min} = 0$ dB, for example. In this scenario, the low-SNR slopes are 1.26 and 2.46 bits/s/Hz per 3 dB with and without the OSTBC input signaling constraint, respectively. Thus, the use of the OSTBC \mathcal{G}_4 incurs about 49% reduction in the slope and, in turn, 49% expansion of the required bandwidth for reliable communication. These slope reduction and bandwidth expansion are much smaller than those for a high-SNR regime: the high-SNR slope for the OSTBC \mathcal{G}_4 is $\mathcal{R} = 3/4$ and the corresponding slope for the general signaling is equal to $\min\{n_T, n_R, n_S\} = 4$ bits/s/Hz per 3 dB [28].

IV. SYMBOL ERROR PROBABILITY

A. Achievable Diversity

Before devoting to deriving the SEP expressions, we discuss the diversity order achieved by the OSTBC. In general, the achievable diversity order can be defined as

$$d \triangleq \lim_{\bar{\gamma} \rightarrow \infty} \frac{-\log P_e}{\log \bar{\gamma}} \quad (56)$$

where P_e denotes the SEP for two-dimensional signaling constellation with polygonal decision boundaries. In the absence of double scattering, the OSTBC provides the maximum achievable diversity order of $n_T n_R$. The corresponding diversity order in double-scattering (n_T, n_R, n_S) -MIMO channels is given by the following result.

Theorem 4: The diversity order achieved by the OSTBC over double-scattering (n_T, n_R, n_S) -MIMO channels is

$$d_{\text{STBC}} = \frac{n_T n_R n_S}{\max \{n_T, n_R, n_S\}}. \quad (57)$$

Proof: We first prove the theorem for M -PSK signaling. For double-scattering (n_T, n_R, n_S) -MIMO channels, the MGF of γ_{STBC} can be written as

$$\begin{aligned} \phi_{\gamma_{\text{STBC}}}(s; \bar{\gamma}) &\triangleq \mathbb{E} \left\{ \text{etr} \left(-\frac{s\bar{\gamma}}{n_T \mathcal{R}} \mathbf{H} \mathbf{H}^\dagger \right) \right\} \\ &= \mathbb{E}_{\Xi_1, \Xi_2} \left\{ \text{etr} \left(-\frac{s\bar{\gamma}}{n_S n_T \mathcal{R}} \Xi_1 \Xi_2 \Xi_2^\dagger \Xi_1^\dagger \right) \right\} \\ &= \mathbb{E}_{\Xi_1} \left\{ \det \left(\mathbf{I}_{n_S n_T} + \frac{s\bar{\gamma}}{n_S n_T \mathcal{R}} \Xi_1^\dagger \Xi_1 \Phi_S \otimes \Phi_T \right)^{-1} \right\} \end{aligned} \quad (58)$$

$$= \mathbb{E}_{\Xi_2} \left\{ \det \left(\mathbf{I}_{n_R n_S} + \frac{s\bar{\gamma}}{n_S n_T \mathcal{R}} \Phi_R \otimes \Xi_2 \Xi_2^\dagger \right)^{-1} \right\} \quad (59)$$

where (58) and (59) follow from Lemma 1 in Appendix II. The SEP of the OSTBC with M -PSK constellation can be expressed as [38], [39]

$$P_{e, \text{MPSK}} = \frac{1}{\pi} \int_0^\Theta \phi_{\gamma_{\text{STBC}}} \left(\frac{g}{\sin^2 \theta}; \bar{\gamma} \right) d\theta \quad (60)$$

where $\Theta = \pi - \pi/M$ and $g = \sin^2(\pi/M)$. From (60), we can obtain the upper bound as

$$P_{e,\text{MPSK}} \leq \left(1 - \frac{1}{M}\right) \phi_{\gamma_{\text{STBC}}}(g; \bar{\gamma}) \quad (61)$$

which becomes tighter as $\bar{\gamma}$ increases [48], and hence yields

$$d_{\text{STBC}} = \lim_{\bar{\gamma} \rightarrow \infty} \frac{-\log \phi_{\gamma_{\text{STBC}}}(g; \bar{\gamma})}{\log \bar{\gamma}}. \quad (62)$$

Therefore, the asymptotic behavior of the MGF $\phi_{\gamma_{\text{STBC}}}(s; \bar{\gamma})$ at large $\bar{\gamma}$ reveals a high-SNR slope of the SEP curve.

Suppose that $\bar{\gamma}$ is sufficiently large. For $n_T \leq n_R$, it follows from (58) that

$$\begin{aligned} \log \phi_{\gamma_{\text{STBC}}}(g; \bar{\gamma}) &\approx \log \mathbb{E} \left\{ \det \left(\frac{g\bar{\gamma}}{n_S n_T \mathcal{R}} \Xi_1^\dagger \Xi_1 \Phi_S \otimes \Phi_T \right)^{-1} \right\} \quad (n_T \leq n_R) \\ &= - \underbrace{\text{rank} \left(\Xi_1^\dagger \Xi_1 \Phi_S \otimes \Phi_T \right)}_{n_T \cdot \min\{n_R, n_S\}} \cdot \log \bar{\gamma} + \text{constant}. \end{aligned} \quad (63)$$

Similarly, using (59), we have for $n_T > n_R$,

$$\begin{aligned} \log \phi_{\gamma_{\text{STBC}}}(g; \bar{\gamma}) &\approx \log \mathbb{E} \left\{ \det \left(\frac{g\bar{\gamma}}{n_S n_T \mathcal{R}} \Phi_R \otimes \Xi_2 \Xi_2^\dagger \right)^{-1} \right\} \quad (n_T > n_R) \\ &= - \underbrace{\text{rank} \left(\Phi_R \otimes \Xi_2 \Xi_2^\dagger \right)}_{n_R \cdot \min\{n_T, n_S\}} \cdot \log \bar{\gamma} + \text{constant}'. \end{aligned} \quad (64)$$

Hence,

$$d_{\text{STBC}} = \min \{n_T, n_R\} \cdot \min \{\max \{n_T, n_R\}, n_S\} \quad (65)$$

from which (57) follows immediately. For a general case of arbitrary two-dimensional signaling constellation with polygonal decision boundaries, the SEP can be written as a convex combination of terms akin to (60) [47], [54]. Hence, we can easily generalize the proof to the case of any two-dimensional signaling constellation. \square

Theorem 4 states that if the number of effective scatterers is greater than or equal to the numbers of transmit and receive antennas, the OSTBC provides the full diversity order of $n_T n_R$ even in the presence of double scattering.

We now present analytical expressions for the SEP of the OSTBC for three cases of particular interest—spatially uncorrelated double scattering, doubly correlated double scattering, and MISO double scattering.

B. Spatially Uncorrelated Double Scattering

Consider a spatial correlation environment $\bar{\Phi}_{\text{uc}} = (\mathbf{I}_{n_T}, \mathbf{I}_{n_R}, \mathbf{I}_{n_S})$. This spatially uncorrelated double-scattering scenario includes i.i.d. and keyhole MIMO channels as special cases.

Let $n_1 = \min\{n_T, n_S\}$, $n_2 = \max\{n_T, n_S\}$, and the $n_1 \times n_1$ random matrix Υ be

$$\Upsilon = \begin{cases} \Xi_2 \Xi_2^\dagger, & \text{if } n_S \leq n_T \\ \Xi_2^\dagger \Xi_2, & \text{if } n_S > n_T, \end{cases} \quad (66)$$

which is a matrix quadratic form in complex Gaussian matrices [28, Definition II.3]. Then, from (59) and (60), the SEP of the OSTBC with M -PSK signaling in double-scattering (n_T, n_R, n_S) -MIMO channels can be readily written as

$$P_{\text{e, MPSK}} = \frac{1}{\pi} \int_0^\Theta \mathbb{E} \left\{ \det \left(\mathbf{I}_{n_1 n_R} + \frac{g\bar{\gamma}}{n_S n_T \mathcal{R} \sin^2 \theta} \Phi_R \otimes \Upsilon \right)^{-1} \right\} d\theta \quad (67)$$

where we have used the fact that $\Xi_2 \Xi_2^\dagger$ and $\Xi_2^\dagger \Xi_2$ have the same nonzero eigenvalues.⁹

In the absence of spatial correlation, the random matrix Υ has the Wishart distribution $\tilde{\mathcal{W}}_{n_1}(n_2, \mathbf{I}_{n_1})$ [28, Definition II.2].¹⁰ Applying Corollary 6 in Appendix II to (67), we obtain the SEP for this spatially uncorrelated environment $\bar{\Phi}_{\text{uc}}$ as

$$P_{\text{e, MPSK}}^{\text{uc-ds}} = \frac{1}{\pi \mathcal{A}^{\text{uc-ds}}} \int_0^\Theta \det \{ \mathbf{G}^{\text{uc-ds}}(\theta) \} d\theta \quad (68)$$

⁹As already mentioned in the proof of Theorem 4, the SEP for the general case of arbitrary two-dimensional signaling constellation with polygonal decision boundaries can be written as a convex combination of terms akin to (60). Thus, our results can be easily extended to any two-dimensional signaling constellation.

¹⁰ $\tilde{\mathcal{W}}_m(n, \Sigma)$ denotes a complex Wishart distribution, where $m \leq n$ and $\Sigma \in \mathbb{C}^{m \times m} > 0$. If $\mathbf{S} \sim \tilde{\mathcal{W}}_m(n, \Sigma)$, then the probability density function (pdf) of \mathbf{S} is given by

$$p_{\mathbf{S}}(\mathbf{S}) = \frac{1}{\tilde{\Gamma}_m(n)} \det(\Sigma)^{-n} \det(\mathbf{S})^{n-m} \text{etr}(-\Sigma^{-1} \mathbf{S}), \quad \mathbf{S} > 0$$

where $\tilde{\Gamma}_m(\alpha) = \pi^{m(m-1)/2} \prod_{i=0}^{m-1} \Gamma(\alpha - i)$ with $\Re(\alpha) > m - 1$ is the complex multivariate gamma function and $\Gamma(\cdot)$ is the gamma function.

where

$$\mathcal{A}^{\text{uc-ds}} = \prod_{k=1}^{n_1} (n_2 - k)! (k - 1)! \quad (69)$$

and $\mathbf{G}^{\text{uc-ds}}(\theta) = (\mathbf{G}_{ij}^{\text{uc-ds}}(\theta))$ is the $n_1 \times n_1$ Hankel matrix whose (i, j) th entry is given by

$$\mathbf{G}_{ij}^{\text{uc-ds}}(\theta) = (n_2 - n_1 + i + j - 2)! {}_2F_0 \left(n_2 - n_1 + i + j - 1, n_R; -\frac{g\bar{\gamma}}{n_S n_T \mathcal{R} \sin^2 \theta} \right). \quad (70)$$

Example 4 (Uncorrelated Extremes—Keyhole and I.I.D.): If $n_S = 1$, then $n_1 = 1$ and $n_2 = n_T$. Hence, (68) reduces to [38, eq. (11)] for keyhole MIMO channels. As $n_S \rightarrow \infty$, (68) becomes [39, eq. (26)] (with a Nakagami parameter $m = 1$) for i.i.d. Rayleigh-fading MIMO channels.

Fig. 4 shows the SEP of 8-PSK \mathcal{G}_4 (2.25 bits/s/Hz) versus the SNR $\bar{\gamma}$ in spatially uncorrelated double-scattering $(4, 2, n_S)$ -MIMO channels when n_S varies from 1 (keyhole) to infinity (i.i.d. Rayleigh). We can see that as n_S increases, the SEP approaches that of i.i.d. Rayleigh-fading MIMO channels in the absence of double scattering. This resembles the behavior in Rayleigh-fading channels with diversity reception, that is, the channel behaves like an AWGN channel (diversity order of ∞) as the number of receive antennas increases. Observe that when $n_S \geq 4$, the slope of the SEP curve at high SNR is identical to that of the i.i.d. case. This example confirms the result of Theorem 4: the diversity orders are equal to $d_{\text{STBC}} = 2, 4$, and 6 for $n_S = 1, 2$, and 3 , respectively, whereas $d_{\text{STBC}} = 8$ for $n_S = 5, 10, 20, 100$, and ∞ (i.i.d.). A clearer understanding about the diversity behavior is obtained by referring to Fig. 5, where the SEPs of 16-PSK Alamouti (4 bits/s/Hz) and \mathcal{G}_4 (3 bits/s/Hz) OSTBCs versus the SNR $\bar{\gamma}$ in spatially uncorrelated double-scattering (n_T, n_R, n_S) -MIMO channels are shown. Using (57), we can easily show that the Alamouti and \mathcal{G}_4 codes achieve the diversity order of $d_{\text{STBC}} = 2$ for $(2, 1, 3)$ and $(4, 1, 2)$ channels; $d_{\text{STBC}} = 6$ for $(2, 3, 5)$ and $(4, 2, 3)$ channels; and $d_{\text{STBC}} = 20$ for $(2, 11, 10)$ and $(4, 5, 5)$ channels. As can be seen, we obtain a close agreement in the slopes of the SEP curves, corresponding to the same value of d_{STBC} , at high SNR.

C. Doubly Correlated Double Scattering

Consider a spatial correlation environment $\bar{\Phi}_{\text{dc}} = (\Phi_T, \Phi_R, \mathbf{I}_{n_S})$, where spatial correlation exists only on the transmit and receive ends. Note that this scenario includes a spatially correlated

MIMO channel in the absence of double scattering ($n_S = \infty$) as a special case. Let λ_i^T and λ_j^R , $i = 1, 2, \dots, n_T$, $j = 1, 2, \dots, n_R$, be the eigenvalues of Φ_T and Φ_R in any order, respectively. Suppose that $n_S \geq n_T$. Then, $\Upsilon \sim \tilde{\mathcal{W}}_{n_T}(n_S, \Phi_T)$. Applying Theorem 10 in Appendix II to (67), we obtain the SEP in the environment $\bar{\Phi}_{dc}$ as

$$P_{s, \text{MPSK}}^{\text{dc-ds}} = \frac{1}{\pi \mathcal{A}^{\text{dc-ds}}} \int_0^\Theta \det \left([\mathbf{G}_1^{\text{dc-ds}}(\theta) \quad \mathbf{G}_2^{\text{dc-ds}}(\theta) \quad \dots \quad \mathbf{G}_{\varrho(\Phi_T)}^{\text{dc-ds}}(\theta)] \right) d\theta \quad (71)$$

with

$$\mathcal{A}^{\text{dc-ds}} = \det \left([\mathbf{B}_1^{\text{dc-ds}} \quad \mathbf{B}_2^{\text{dc-ds}} \quad \dots \quad \mathbf{B}_{\varrho(\Phi_T)}^{\text{dc-ds}}] \right) \cdot \prod_{i=1}^{n_T} (n_S - i)! \quad (72)$$

where $\mathbf{B}_k^{\text{dc-ds}} = (\mathbf{B}_{k,ij}^{\text{dc-ds}})$ and $\mathbf{G}_k^{\text{dc-ds}}(\theta) = (\mathbf{G}_{k,ij}^{\text{dc-ds}}(\theta))$, $k = 1, 2, \dots, \varrho(\Phi_T)$, are $n_T \times \ell_k(\Phi_T)$ matrices whose (i, j) th entries are given respectively by

$$\mathbf{B}_{k,ij}^{\text{dc-ds}} = (-1)^{i-j} (i - j + 1)_{j-1} \lambda_{\langle k \rangle}^T n_S^{-i+j} \quad (73)$$

and

$$\begin{aligned} \mathbf{G}_{k,ij}^{\text{dc-ds}}(\theta) = \sum_{p=1}^{\varrho(\Phi_R)} \sum_{q=1}^{\ell_p(\Phi_R)} \left\{ \mathcal{X}_{p,q}(\Phi_R) \cdot \lambda_{\langle k \rangle}^T n_S^{-n_T+i+j-1} (n_S - n_T + i + j - 2)! \right. \\ \left. \times {}_2F_0 \left(n_S - n_T + i + j - 1, q; -\frac{g\bar{\gamma}\lambda_{\langle p \rangle}^R \lambda_{\langle k \rangle}^T}{n_S n_T \mathcal{R} \sin^2 \theta} \right) \right\}. \end{aligned} \quad (74)$$

In (74), $\mathcal{X}_{p,q}(\Phi_R)$ is the (p, q) th characteristic coefficient of Φ_R (see Definition 6 in Appendix II).

Fig. 6 shows the SEP of 8-PSK \mathcal{G}_4 versus the SNR $\bar{\gamma}$ in doubly correlated double-scattering $(4, 4, 10)$ -MIMO channels. In this figure, the transmit and receive correlations follow the constant correlation, defined in (82), $\Phi_T = \Phi_R = \Phi_4^{(c)}(\rho)$ and the correlation coefficient ρ ranges from 0 (spatially uncorrelated double scattering) to 0.9. The characteristic coefficients of the constant correlation matrix are given by (170) and (171) (see Example 6 in Appendix II). For comparison, we also plot the SEP of i.i.d. Rayleigh-fading MIMO channels. In Figure 6, we can see that the SNR penalty due to double scattering with $n_S = 10$ (in the absence of spatial correlation) is about 1 dB at the SEP of 10^{-6} and it becomes larger than 2.5 dB for $\rho \geq 0.5$. In Fig. 7, the SEP of 8-PSK \mathcal{G}_4 at $\bar{\gamma} = 15$ dB is depicted as a function of a correlation coefficient ρ for doubly correlated double-scattering $(4, 4, n_S)$ -MIMO channels with constant correlation $\Phi_T = \Phi_R = \Phi_4^{(c)}(\rho)$ when

$n_S = 5, 10, 20, 50, 100$, and ∞ (doubly correlated Rayleigh). This figure demonstrates that double scattering and spatial correlation degrade the SEP performance considerably.

D. MISO Double Scattering

Finally, we consider a double-scattering MISO channel. This is a pure transmit diversity system wherein the burden of diversity reception at the receive terminal is moved to the transmitter.

The SEP in double-scattering MISO channels can be obtained from (59) with $n_R = 1$ as

$$P_{\text{e, MPSK}}^{\text{miso-ds}} = \frac{1}{\pi} \int_0^\Theta \mathbb{E} \left\{ \det \left(\mathbf{I}_{n_S} + \frac{g\bar{\gamma}}{n_S n_T \mathcal{R} \sin^2 \theta} \mathbf{\Xi}_2 \mathbf{\Xi}_2^\dagger \right)^{-1} \right\} d\theta. \quad (75)$$

Let λ_i^S , $i = 1, 2, \dots, n_S$, be the eigenvalues of $\mathbf{\Phi}_S$ in any order. Then, applying Theorem 11 in Appendix II to (75), we obtain

$$P_{\text{e, MPSK}}^{\text{miso-ds}} = \frac{1}{\pi} \sum_{p=1}^{\varrho(\mathbf{\Phi}_S)} \sum_{q=1}^{\varrho(\mathbf{\Phi}_T)} \sum_{i=1}^{\ell_p(\mathbf{\Phi}_S)} \sum_{j=1}^{\ell_q(\mathbf{\Phi}_T)} \mathcal{X}_{p,i}(\mathbf{\Phi}_S) \mathcal{X}_{q,j}(\mathbf{\Phi}_T) \int_0^\Theta {}_2F_0 \left(i, j; -\frac{g\bar{\gamma} \lambda_{\langle p \rangle}^S \lambda_{\langle q \rangle}^T}{n_S n_T \mathcal{R} \sin^2 \theta} \right) d\theta \quad (76)$$

where $\mathcal{X}_{p,i}(\mathbf{\Phi}_S)$ and $\mathcal{X}_{q,j}(\mathbf{\Phi}_T)$ are the characteristic coefficients of $\mathbf{\Phi}_S$ and $\mathbf{\Phi}_T$, respectively.

The effects of the spatial correlation and the number of effective scatterers on the SEP performance in MISO channels can be ascertained by referring to Fig. 8, where the SEP of 8-PSK \mathcal{G}_4 at $\bar{\gamma} = 25$ dB versus n_S is depicted for double-scattering $(4, 1, n_S)$ -MIMO channels. The transmit and scatterer correlations follow the constant correlation $\mathbf{\Phi}_T = \mathbf{\Phi}_4^{(c)}(\rho)$ and $\mathbf{\Phi}_S = \mathbf{\Phi}_{n_S}^{(c)}(\rho)$ where ρ varies from 0 to 0.9. Note that the maximum achievable diversity order is equal to $d_{\text{STBC}} = 4$ for $n_S \geq 4$. Hence, the SEP performance improves rapidly as n_S increases, and approaches the corresponding SEP in the absence of double scattering.

V. CONCLUSIONS

We investigated the combined effect of rank deficiency and spatial fading correlation on the diversity performance of MIMO systems. In particular, we considered double-scattering MIMO channels employing OSTBCs which use up all antennas to realize full diversity advantage. We characterized the effects of double scattering on the severity of fading and the low-SNR capacity by quantifying the EFF and the capacity slope in terms of the *correlation figures* of spatial correlation matrices. The Schur monotonicity properties were shown for these performance

measures as functionals of the eigenvalues of correlation matrices. We also determined the required richness of the channel to achieve the full diversity order of $n_T n_R$. Finally, we derived the exact SEP expressions for the cases of spatially uncorrelated/doubly correlated/MISO double scattering, which consolidate the effects of rank efficiency and spatial correlation on the SEP performance.

APPENDIX I

MAJORIZATION, SCHUR MONOTONICITY, AND CORRELATION MATRICES

We use the concept of majorization [55]–[59] as a mathematical tool to characterize different spatial correlation environments. Using the majorization theory, the analytical framework was established in [44] to assess the performance of multiple-antenna diversity systems with different *power dispersion profiles*. In particular, monotonicity theorems were proved for various performance measures such as the NSD of the output SNR, the ergodic capacity, the matched-filter bound, the inverse SEP, and the symbol error outage. The notion of majorization has also been used in [25], [33], [60] as a measure of correlation. In this appendix, we briefly discuss the basic properties of majorization and Schur monotonicity.

A. Majorization and Correlation Matrices

Given a real vector $\mathbf{a} = (a_1, a_2, \dots, a_n)^T \in \mathbb{R}^n$, we rearrange its components in decreasing order as $a_{[1]} \geq a_{[2]} \geq \dots \geq a_{[n]}$.

Definition 4: For $\mathbf{a} = (a_1, a_2, \dots, a_n)^T, \mathbf{b} = (b_1, b_2, \dots, b_n)^T \in \mathbb{R}^n$, we denote $\mathbf{a} \prec \mathbf{b}$ and say that \mathbf{a} is *weakly majorized* (or *submajorized*) by \mathbf{b} if

$$\sum_{i=1}^k a_{[i]} \leq \sum_{i=1}^k b_{[i]}, \quad k = 1, 2, \dots, n. \quad (77)$$

If $\sum_{i=1}^n a_i = \sum_{i=1}^n b_i$ holds in addition to $\mathbf{a} \prec \mathbf{b}$, then we say that \mathbf{a} is *majorized* by \mathbf{b} and denote as $\mathbf{a} \preceq \mathbf{b}$.

For example, if each $a_i \geq 0$ and $\sum_{i=1}^n a_i = n$, then

$$(1, 1, \dots, 1)^T \preceq (a_1, a_2, \dots, a_n)^T \preceq (n, 0, \dots, 0)^T. \quad (78)$$

Of particular interest are the majorization relations among Hermitian matrices in terms of their eigenvalue vectors to compare different spatial correlation environments. A Hermitian matrix \mathbf{A} is said to be *majorized* by a Hermitian matrix \mathbf{B} , simply denoted by $\mathbf{A} \preceq \mathbf{B}$, if $\lambda(\mathbf{A}) \preceq \lambda(\mathbf{B})$ where $\lambda(\cdot)$ denote the vector of eigenvalues of a Hermitian matrix. For example, the well-known Schur's theorem [58, eq. (5.5.8)] on the relationship between the eigenvalues and diagonal entries of Hermitian matrices can be written as

$$\mathbf{A} \circ \mathbf{I}_n \preceq \mathbf{A} \quad \text{for Hermitian } \mathbf{A} \in \mathbb{C}^{n \times n} \quad (79)$$

where \circ denotes a Hadamard (i.e., entrywise) product. One of the most useful results on the eigenvalue majorization is the following theorem.

Theorem 5 ([57, Theorem 7.1]): A linear map $\mathcal{L} : \mathbb{C}^{n \times n} \rightarrow \mathbb{C}^{n \times n}$ is called *positive* if $\mathcal{L}(\mathbf{A}) \geq 0$ for $\mathbf{A} \in \mathbb{C}^{n \times n} \geq 0$ and *unital* if $\mathcal{L}(\mathbf{I}_n) = \mathbf{I}_n$. It is said to be *doubly stochastic* if \mathcal{L} is a unital positive linear map with the trace-preserving property, i.e., $\text{tr } \mathcal{L}(\mathbf{A}) = \text{tr}(\mathbf{A})$, $\forall \mathbf{A} \in \mathbb{C}^{n \times n}$. Let $\mathbf{A} \in \mathbb{C}^{n \times n}$ be Hermitian and \mathcal{L} be a doubly stochastic map. Then,

$$\mathcal{L}(\mathbf{A}) \preceq \mathbf{A}. \quad (80)$$

Recall that the Schur product theorem [58, Theorem 5.2.1] says that the Hadamard product of two positive semidefinite matrices is positive semidefinite. Therefore if $\Phi \in \mathbb{C}^{n \times n}$ is an arbitrary correlation matrix and define $\mathcal{L}(\mathbf{A}) = \mathbf{A} \circ \Phi$, then \mathcal{L} is obviously a doubly stochastic map on $\mathbb{C}^{n \times n}$.

Corollary 3: Let $\mathbf{A} \in \mathbb{C}^{n \times n}$ be Hermitian and $\Phi \in \mathbb{C}^{n \times n}$ be a correlation matrix. Then,

$$\mathbf{A} \circ \Phi \preceq \mathbf{A}. \quad (81)$$

In fact, this result was first given in [59, Corollary 2] without using the notion of doubly stochastic maps. From Corollary 3, we can obtain the eigenvalue majorization relations for the well-known correlation models—*constant*, *exponential*, and *tridiagonal correlation*—which have been widely used for many communication problems of multiple-antenna systems (see, e.g., [28]–[30], [46], [48], [61]–[63]).

Example 5 (Constant, Exponential, and Tridiagonal Matrices): The n th-order constant, exponential, and tridiagonal matrices with a coefficient ρ , denoted by $\Phi_n^{(c)}(\rho)$, $\Phi_n^{(e)}(\rho)$, and $\Phi_n^{(t)}(\rho)$ respectively, are $n \times n$ symmetric Toeplitz matrices of the following structures:

$$\Phi_n^{(c)}(\rho) = \begin{bmatrix} 1 & \rho & \rho & \cdots & \rho \\ \rho & 1 & \rho & \cdots & \rho \\ \vdots & \vdots & \vdots & \ddots & \vdots \\ \rho & \rho & \rho & \cdots & 1 \end{bmatrix}_{n \times n} \quad (82)$$

$$\Phi_n^{(e)}(\rho) = \begin{bmatrix} 1 & \rho & \rho^2 & \cdots & \rho^{(n-1)} \\ \rho & 1 & \rho & \cdots & \rho^{(n-2)} \\ \vdots & \vdots & \vdots & \ddots & \vdots \\ \rho^{n-1} & \rho^{n-2} & \rho^{n-3} & \cdots & 1 \end{bmatrix}_{n \times n} \quad (83)$$

and

$$\Phi_n^{(t)}(\rho) = \begin{bmatrix} 1 & \rho & & & 0 \\ \rho & 1 & \rho & & \\ & \rho & 1 & \rho & \\ & & \ddots & \ddots & \ddots \\ 0 & & & \rho & 1 & \rho \\ & & & \rho & 1 & 1 \end{bmatrix}_{n \times n}. \quad (84)$$

Note that $\Phi_n^{(c)}(\rho)$, $\Phi_n^{(e)}(\rho)$ with $\rho \in [0, 1]$ and $\Phi_n^{(t)}(\rho)$ with $\rho \in [0, 0.5 / \cos \frac{\pi}{n+1}]$ are correlation matrices, since they are positive semidefinite for such values of ρ . Let $0 \leq \rho_1 \leq \rho_2$. Then, since

$$\Phi_n^{(c)}(\rho_1) = \Phi_n^{(c)}(\rho_2) \circ \Phi_n^{(c)}\left(\frac{\rho_1}{\rho_2}\right)$$

$$\Phi_n^{(e)}(\rho_1) = \Phi_n^{(e)}(\rho_2) \circ \Phi_n^{(e)}\left(\frac{\rho_1}{\rho_2}\right)$$

$$\Phi_n^{(t)}(\rho_1) = \Phi_n^{(t)}(\rho_2) \circ \Phi_n^{(e)}\left(\frac{\rho_1}{\rho_2}\right),$$

it follows from Corollary 3 that

$$\Phi_n^{(c)}(\rho_1) \preceq \Phi_n^{(c)}(\rho_2) \quad (85)$$

$$\Phi_n^{(e)}(\rho_1) \preceq \Phi_n^{(e)}(\rho_2) \quad (86)$$

$$\Phi_n^{(t)}(\rho_1) \preceq \Phi_n^{(t)}(\rho_2). \quad (87)$$

Remark: If $0 \leq \rho_1 \leq \rho_2$, then $\Phi_n^{(c)}\left(\frac{\rho_1}{\rho_2}\right)$ and $\Phi_n^{(e)}\left(\frac{\rho_1}{\rho_2}\right)$ are positive semidefinite. Hence, the majorization relations (85)–(87) hold, although each matrix itself is only Hermitian but may not be positive semidefinite.

B. Schur Monotonicity

The concept of majorization is closely related to a MIS (or MDS) function. If a function $f : (\text{a subset of}) \mathbb{R}^n \rightarrow \mathbb{R}$ satisfies $f(a_1, \dots, a_n) \leq f(b_1, \dots, b_n)$ whenever $\mathbf{a} \preceq \mathbf{b}$, then f is called a MIS (or isotone) function on (a subset of) \mathbb{R}^n . The following theorem gives a necessary and sufficient condition for f to be MIS.

Theorem 6 (Schur 1923): Let $\mathbb{I} \subset \mathbb{R}$ and $f : \mathbb{I}^n \rightarrow \mathbb{R}$ be continuously differentiable. Then, the function f is MIS on \mathbb{I}^n if and only if

$$f \text{ is symmetric on } \mathbb{I}^n \quad (88)$$

and for all $i \neq j$,

$$(a_i - a_j) \left[\frac{\partial f}{\partial a_i} - \frac{\partial f}{\partial a_j} \right] \geq 0 \quad \forall \mathbf{a} \in \mathbb{I}^n. \quad (89)$$

Note that Schur's condition (89) can be replaced by

$$(a_1 - a_2) \left[\frac{\partial f}{\partial a_1} - \frac{\partial f}{\partial a_2} \right] \geq 0 \quad \forall \mathbf{a} \in \mathbb{I}^n \quad (90)$$

because of the symmetry. If f is MIS on \mathbb{I}^n , then $-f$ is a MDS function on \mathbb{I}^n .

Corollary 4 (Correlation Figure): Let Φ be an $n \times n$ correlation matrix. Then, the correlation figure $\zeta(\Phi)$ as a functional of the eigenvalues of Φ is MIS, that is, if $\Phi_1 \preceq \Phi_2$, then

$$\zeta(\Phi_1) \leq \zeta(\Phi_2). \quad (91)$$

Proof: Let $\lambda_1, \lambda_2, \dots, \lambda_n$ be the eigenvalues of Φ . Then, the correlation figure $\zeta(\Phi)$ defined in Definition 1 can be written as

$$\zeta(\Phi) = \frac{1}{n^2} \sum_{k=1}^n \lambda_k^2 \quad (92)$$

which is symmetric in $\lambda_1, \lambda_2, \dots, \lambda_n$ and holds Schur's condition (90). Hence, we complete the proof. \square

APPENDIX II

COMPLEX GAUSSIAN MATRICES

This appendix gives useful results on some statistics derived from complex Gaussian matrices. In our derivations, we will make extensive use of the following elementary properties of the Kronecker product and vectorization operator (see, e.g., [58]):

- 1) For any conformable complex matrices \mathbf{A} , \mathbf{B} , \mathbf{C} , and \mathbf{D} , we have

$$\text{tr}(\mathbf{ABCD}) = (\text{vec}(\mathbf{B}^\dagger))^\dagger (\mathbf{A}^T \otimes \mathbf{C}) \text{vec}(\mathbf{D}) \quad (93)$$

$$(\mathbf{A} \otimes \mathbf{B})(\mathbf{C} \otimes \mathbf{D}) = \mathbf{AC} \otimes \mathbf{BD}. \quad (94)$$

- 2) For any $m \times m$ complex matrix \mathbf{A} with eigenvalues λ_i , $i = 1, 2, \dots, m$, and $n \times n$ complex matrix \mathbf{B} with eigenvalues μ_j , $j = 1, 2, \dots, n$, the eigenvalues of $\mathbf{A} \otimes \mathbf{B}$ are

$$\lambda_i \mu_j, \quad i = 1, 2, \dots, m, \quad j = 1, 2, \dots, n \quad (95)$$

and hence,

$$\text{tr}(\mathbf{A} \otimes \mathbf{B}) = \text{tr}(\mathbf{A}) \text{tr}(\mathbf{B}) \quad (96)$$

$$\det(\mathbf{A} \otimes \mathbf{B}) = \det(\mathbf{A})^n \det(\mathbf{B})^m. \quad (97)$$

A. Definition and Preliminary Results

We begin by giving the definition and distribution of complex Gaussian matrices. Let us denote a complex n -variate Gaussian distribution with a mean vector $\boldsymbol{\mu} \in \mathbb{C}^n$ and a covariance matrix $\boldsymbol{\Sigma} \in \mathbb{C}^{n \times n}$ by $\tilde{\mathcal{N}}_n(\boldsymbol{\mu}, \boldsymbol{\Sigma})$.

Definition 5 (Complex Gaussian Matrix): A random matrix $\mathbf{X} \in \mathbb{C}^{m \times n}$ is said to have a matrix-variate Gaussian distribution with mean matrix $\mathbf{M} \in \mathbb{C}^{m \times n}$ and covariance matrix $\boldsymbol{\Sigma}^T \otimes \boldsymbol{\Psi}$, where $\boldsymbol{\Sigma} \in \mathbb{C}^{m \times m} > 0$ and $\boldsymbol{\Psi} \in \mathbb{C}^{n \times n} > 0$ are Hermitian, if

$$\text{vec}(\mathbf{X}^\dagger) \sim \tilde{\mathcal{N}}_{mn}(\text{vec}(\mathbf{M}^\dagger), \boldsymbol{\Sigma}^T \otimes \boldsymbol{\Psi}).$$

We shall use the notation $\mathbf{X} \sim \tilde{\mathcal{N}}_{m,n}(\mathbf{M}, \boldsymbol{\Sigma}, \boldsymbol{\Psi})$ to denote that \mathbf{X} is (matrix variate) Gaussian distributed. The probability density function (pdf) of \mathbf{X} is given by

$$p_{\mathbf{X}}(\mathbf{X}) = \pi^{-mn} \det(\boldsymbol{\Sigma})^{-n} \det(\boldsymbol{\Psi})^{-m} \text{etr} \left\{ -\boldsymbol{\Sigma}^{-1} (\mathbf{X} - \mathbf{M}) \boldsymbol{\Psi}^{-1} (\mathbf{X} - \mathbf{M})^\dagger \right\}. \quad (98)$$

It should be noted that $\mathbf{X}^\dagger \sim \tilde{\mathcal{N}}_{n,m}(\mathbf{M}^\dagger, \mathbf{\Psi}, \mathbf{\Sigma})$.

Lemma 1: Let $\mathbf{X}_k \sim \tilde{\mathcal{N}}_{m,n}(\mathbf{0}_{m \times n}, \mathbf{\Sigma}, \mathbf{\Psi}_k)$, $k = 1, 2, \dots, p$, be statistically independent complex Gaussian matrices and¹¹

$$\mathbf{X} = [\mathbf{X}_1 \ \mathbf{X}_2 \ \cdots \ \mathbf{X}_p] \sim \tilde{\mathcal{N}}_{m,np}(\mathbf{0}_{m \times np}, \mathbf{\Sigma}, \mathbf{\Psi}_1 \oplus \mathbf{\Psi}_2 \oplus \cdots \oplus \mathbf{\Psi}_p). \quad (99)$$

Then, for $\mathbf{A} \in \mathbb{C}^{m \times m} \geq 0$ and $\mathbf{B} = \mathbf{B}_1 \oplus \mathbf{B}_2 \oplus \cdots \oplus \mathbf{B}_p$, $\mathbf{B}_k \in \mathbb{C}^{n \times n} \geq 0$, we have

$$\mathbb{E} \left\{ \text{etr}(-\mathbf{A}\mathbf{X}\mathbf{B}\mathbf{X}^\dagger) \right\} = \prod_{k=1}^p \det(\mathbf{I}_{mn} + \mathbf{A}\mathbf{\Sigma} \otimes \mathbf{\Psi}_k \mathbf{B}_k)^{-1}. \quad (100)$$

Proof: Since $\mathbf{A}\mathbf{X}\mathbf{B}\mathbf{X}^\dagger = \sum_{k=1}^p \mathbf{A}\mathbf{X}_k \mathbf{B}_k \mathbf{X}_k^\dagger$, we have

$$\mathbb{E} \left\{ \text{etr}(-\mathbf{A}\mathbf{X}\mathbf{B}\mathbf{X}^\dagger) \right\} = \prod_{k=1}^p \mathbb{E}_{\mathbf{X}_k} \left\{ \text{etr}(-\mathbf{A}\mathbf{X}_k \mathbf{B}_k \mathbf{X}_k^\dagger) \right\}. \quad (101)$$

Therefore¹²

$$\begin{aligned} & \mathbb{E}_{\mathbf{X}_k} \left\{ \text{etr}(-\mathbf{A}\mathbf{X}_k \mathbf{B}_k \mathbf{X}_k^\dagger) \right\} \\ & \stackrel{(a)}{=} c_k \int_{\mathbf{X}_k} \text{etr}(-\mathbf{A}\mathbf{X}_k \mathbf{B}_k \mathbf{X}_k^\dagger - \mathbf{\Sigma}^{-1} \mathbf{X}_k \mathbf{\Psi}_k^{-1} \mathbf{X}_k^\dagger) d\mathbf{X}_k \\ & \stackrel{(b)}{=} c_k \int_{\mathbf{X}_k} \exp \left[-(\text{vec}(\mathbf{X}_k^\dagger))^\dagger \left\{ (\mathbf{\Sigma}^T \otimes \mathbf{\Psi}_k)^{-1} + \mathbf{A}^T \otimes \mathbf{B}_k \right\} \text{vec}(\mathbf{X}_k^\dagger) \right] d\mathbf{X}_k \\ & = c_k \pi^{mn} \det \left\{ (\mathbf{\Sigma}^T \otimes \mathbf{\Psi}_k)^{-1} + \mathbf{A}^T \otimes \mathbf{B}_k \right\}^{-1} \\ & \stackrel{(c)}{=} \det(\mathbf{I}_{mn} + \mathbf{A}\mathbf{\Sigma} \otimes \mathbf{\Psi}_k \mathbf{B}_k)^{-1} \end{aligned} \quad (102)$$

where $c_k = \pi^{-mn} \det(\mathbf{\Sigma})^{-n} \det(\mathbf{\Psi}_k)^{-m}$, (a) follows from the pdf (98), (b) follows from the property (93), and (c) follows from the properties (94), (97), and the fact that $\mathbf{\Sigma}^T \mathbf{A}^T$ and $\mathbf{A}\mathbf{\Sigma}$ have the same eigenvalues. Combining (101) and (102) complete the proof. \square

¹¹ $\mathbf{A} \oplus \mathbf{B} = \begin{bmatrix} \mathbf{A} & \mathbf{0} \\ \mathbf{0} & \mathbf{B} \end{bmatrix}$ denotes a direct sum of matrices \mathbf{A} and \mathbf{B} .

¹²If $\mathbf{X} = (X_{ij})$ is an $m \times n$ matrix of functionally independent complex variables, then

$$d\mathbf{X} = \prod_{i=1}^m \prod_{j=1}^n d\Re X_{ij} d\Im X_{ij}.$$

Lemma 2: Let $\mathbf{X} \sim \tilde{\mathcal{N}}_{m,n}(\mathbf{0}_{m \times n}, \mathbf{\Sigma}, \mathbf{\Psi})$. Then, for $\mathbf{A}, \mathbf{B} \in \mathbb{C}^{m \times n}$, we have

$$\mathbb{E} \left\{ \text{etr}(\mathbf{X}^\dagger \mathbf{A} + \mathbf{B}^\dagger \mathbf{X}) \right\} = \text{etr}(\mathbf{\Sigma} \mathbf{A} \mathbf{\Psi} \mathbf{B}^\dagger). \quad (103)$$

Proof: Let \mathbf{M}_1 and \mathbf{M}_2 be $m \times n$ matrices such that

$$\begin{aligned} & \text{tr}(\mathbf{X}^\dagger \mathbf{A} + \mathbf{B}^\dagger \mathbf{X} - \mathbf{\Sigma}^{-1} \mathbf{X} \mathbf{\Psi}^{-1} \mathbf{X}^\dagger) \\ &= \text{tr}(\mathbf{\Sigma}^{-1} \mathbf{M}_1 \mathbf{\Psi}^{-1} \mathbf{M}_2^\dagger) + \text{tr} \left\{ -\mathbf{\Sigma}^{-1} (\mathbf{X} - \mathbf{M}_1) \mathbf{\Psi}^{-1} (\mathbf{X} - \mathbf{M}_2)^\dagger \right\}. \end{aligned} \quad (104)$$

Then, since

$$\int_{\mathbf{X}} \text{etr} \left\{ -\mathbf{\Sigma}^{-1} (\mathbf{X} - \mathbf{M}_1) \mathbf{\Psi}^{-1} (\mathbf{X} - \mathbf{M}_2)^\dagger \right\} d\mathbf{X} = \pi^{mn} \det(\mathbf{\Sigma})^n \det(\mathbf{\Psi})^m, \quad (105)$$

we get

$$\mathbb{E} \left\{ \text{etr}(\mathbf{X}^\dagger \mathbf{A} + \mathbf{B}^\dagger \mathbf{X}) \right\} = \text{etr}(\mathbf{\Sigma}^{-1} \mathbf{M}_1 \mathbf{\Psi}^{-1} \mathbf{M}_2^\dagger). \quad (106)$$

By comparing both the sides of (104), we have

$$\mathbf{M}_1 = \mathbf{\Sigma} \mathbf{A} \mathbf{\Psi} \quad (107)$$

$$\mathbf{M}_2 = \mathbf{\Sigma} \mathbf{B} \mathbf{\Psi} \quad (108)$$

Finally, substituting (107) and (108) into (106) completes the proof. \square

Lemma 3: Let $\mathbf{X} \sim \tilde{\mathcal{N}}_{m,n}(\mathbf{M}, \mathbf{\Sigma}, \mathbf{\Psi})$. Then, the characteristic function of \mathbf{X} is

$$\begin{aligned} \Phi_{\mathbf{X}}(\mathbf{Z}) &\triangleq \mathbb{E} \left\{ \exp \left[j \Re \text{tr}(\mathbf{X} \mathbf{Z}^\dagger) \right] \right\} \\ &= \exp \left[j \Re \text{tr}(\mathbf{M} \mathbf{Z}^\dagger) - \frac{1}{4} \text{tr}(\mathbf{\Sigma} \mathbf{Z} \mathbf{\Psi} \mathbf{Z}^\dagger) \right] \end{aligned} \quad (109)$$

where $j = \sqrt{-1}$ and $\mathbf{Z} \in \mathbb{C}^{m \times n}$ is an arbitrary matrix.

Proof: Let $\mathbf{X}_1 \sim \tilde{\mathcal{N}}_{m,n}(\mathbf{0}_{m \times n}, \mathbf{\Sigma}, \mathbf{\Psi})$. Then,

$$\Phi_{\mathbf{X}}(\mathbf{Z}) = \exp \left[j \Re \text{tr}(\mathbf{M} \mathbf{Z}^\dagger) \right] \cdot \mathbb{E} \left\{ \exp \left[j \Re \text{tr}(\mathbf{X}_1 \mathbf{Z}^\dagger) \right] \right\}. \quad (110)$$

Since

$$\Re \text{tr}(\mathbf{X}_1 \mathbf{Z}^\dagger) = \frac{1}{2} \text{tr}(\mathbf{Z}^\dagger \mathbf{X}_1 + \mathbf{X}_1^\dagger \mathbf{Z}), \quad (111)$$

it follows from Lemma 2 that

$$\mathbb{E} \left\{ \exp \left[j \Re \operatorname{tr} (\mathbf{X}_1 \mathbf{Z}^\dagger) \right] \right\} = \operatorname{etr} \left(-\frac{1}{4} \boldsymbol{\Sigma} \mathbf{Z} \boldsymbol{\Psi} \mathbf{Z}^\dagger \right). \quad (112)$$

Combining (110) and (112) completes the proof. \square

We remark that Lemma 3 is a counterpart result of the real case in [64, Theorem 2.3.2].

B. Hypergeometric Functions of Matrix Arguments

The hypergeometric functions of matrix arguments often appear in deriving the distributions and statistics of random matrices [64]–[68]. In parallel to the hypergeometric functions of a scalar argument, the hypergeometric functions of one or two matrix arguments can be expressed as an infinite series of zonal polynomials¹³:

$${}_p \tilde{F}_q (a_1, \dots, a_p; b_1, \dots, b_q; \mathbf{A}) = \sum_{k=0}^{\infty} \sum_{\kappa} \frac{[a_1]_{\kappa} \cdots [a_p]_{\kappa}}{[b_1]_{\kappa} \cdots [b_q]_{\kappa}} \frac{\tilde{C}_{\kappa}(\mathbf{A})}{k!} \quad (113)$$

$${}_p \tilde{F}_q^{(n)} (a_1, \dots, a_p; b_1, \dots, b_q; \mathbf{A}, \mathbf{B}) = \sum_{k=0}^{\infty} \sum_{\kappa} \frac{[a_1]_{\kappa} \cdots [a_p]_{\kappa}}{[b_1]_{\kappa} \cdots [b_q]_{\kappa}} \frac{\tilde{C}_{\kappa}(\mathbf{A}) \tilde{C}_{\kappa}(\mathbf{B})}{k! \tilde{C}_{\kappa}(\mathbf{I}_n)} \quad (114)$$

with Hermitian $\mathbf{A} \in \mathbb{C}^{n \times n}$ and $\mathbf{B} \in \mathbb{C}^{n \times n}$. In (113) and (114), $\kappa = (k_1, k_2, \dots, k_n)$ denotes a partition of the nonnegative integer k such that $k_1 \geq k_2 \geq \dots \geq k_n \geq 0$ and $\sum_{i=1}^n k_i = k$, $[a]_{\kappa}$ is the complex multivariate hypergeometric coefficient of the partition κ [66, eq. (84)], and $\tilde{C}_{\kappa}(\cdot)$ is the zonal polynomial of a Hermitian matrix [66, eq. (85)]. Although these functions are of great interest from an analytical point of view, the practical difficulty lies in their numerical aspects. The determinantal representation for the hypergeometric function of two Hermitian matrices [68, Lemma 3] settles this computational problem and has been widely used in the literature of multiple-antenna communication theory (see, e.g., [29], [30], [49], [50]). However, [68, Lemma 3] is valid only for the case of two matrix arguments with the same dimension

¹³Zonal polynomials of a symmetric matrix were introduced in [65] using group representation theory. In parallel to a real matrix argument, zonal polynomials of a Hermitian matrix were defined in [66] as natural extension of the real case. Those polynomials are homogeneous symmetric functions in the eigenvalues of matrix argument and can be constructed in terms of homogeneous symmetric polynomials such as monomial symmetric functions, elementary symmetric functions, and Schur functions [69].

and the distinct eigenvalues. In the following lemma, we generalize [68, Lemma 3] for the case that two matrix arguments have the different matrix dimension and the eigenvalues of arbitrary multiplicity.

Lemma 4 (Generic Determinantal Formula): Let $\mathbf{\Lambda} \in \mathbb{C}^{m \times m}$ and $\mathbf{\Sigma} \in \mathbb{C}^{n \times n}$, $m \leq n$, be Hermitian matrices with the ordered eigenvalues $\lambda_1 \geq \lambda_2 \geq \dots \geq \lambda_m$ and $\sigma_1 \geq \sigma_2 \geq \dots \geq \sigma_n$, respectively. Given $a_i, b_j \in \mathbb{C}$ where $i = 1, 2, \dots, p$ and $j = 1, 2, \dots, q$, define

$$\mathcal{H}_{p,q}^{n,\nu}(x) \triangleq {}_pF_q(a_1 - n + \nu, \dots, a_p - n + \nu; b_1 - n + \nu, \dots, b_q - n + \nu; x) \quad (115)$$

$$\chi_{p,q}^{n,\nu} \triangleq \frac{\prod_{j=1}^q (b_j - n + 1)_\nu}{\prod_{i=1}^p (a_i - n + 1)_\nu} \quad (116)$$

where ν is an arbitrary nonnegative integer, $(a)_n = a(a+1)\cdots(a+n-1)$, $(a)_0 = 1$ is the Pochhammer symbol, and ${}_pF_q(a_1, a_2, \dots, a_p; b_1, b_2, \dots, b_q; z)$ is the generalized hypergeometric function of scalar argument [70, eq. (9.14.1)]. Then,

$$\begin{aligned} & {}_p\tilde{F}_q^{(n)}(a_1, \dots, a_p; b_1, \dots, b_q; \mathbf{\Lambda}, \mathbf{\Sigma}) \cdot \prod_{i < j}^m (\lambda_j - \lambda_i) \\ &= \frac{K_{p,q}^{m,n}}{\det(\mathbf{\Lambda})^{n-m}} \cdot \frac{\det \left(\begin{bmatrix} \mathbf{Z}^{(n-m),1} & \mathbf{Z}^{(n-m),2} & \cdots & \mathbf{Z}^{(n-m),\varrho(\mathbf{\Sigma})} \\ \mathbf{Y}_1 & \mathbf{Y}_2 & \cdots & \mathbf{Y}_{\varrho(\mathbf{\Sigma})} \end{bmatrix} \right)}{\det \left(\begin{bmatrix} \mathbf{Z}_{(n),1} & \mathbf{Z}_{(n),2} & \cdots & \mathbf{Z}_{(n),\varrho(\mathbf{\Sigma})} \end{bmatrix} \right)} \end{aligned} \quad (117)$$

with

$$K_{p,q}^{m,n} = \prod_{i=1}^m \chi_{p,q}^{n,n-i} \cdot (n-i)! \quad (118)$$

where $\mathbf{Y}_k = (\mathcal{Y}_{k,ij})$ and $\mathbf{Z}_{(l),k} = (\mathcal{Z}_{(l),k,ij})$, $l \leq n$, $k = 1, 2, \dots, \varrho(\mathbf{\Sigma})$, are $m \times \ell_k(\mathbf{\Sigma})$ and $l \times \ell_k(\mathbf{\Sigma})$ matrices, whose (i, j) th entries are given respectively by

$$\mathcal{Y}_{k,ij} = \frac{\lambda_i^{j-1}}{\chi_{p,q}^{n,j-1}} \cdot \mathcal{H}_{p,q}^{n,j}(\lambda_i \sigma_{\langle k \rangle}) \quad (119)$$

$$\mathcal{Z}_{(l),k,ij} = (i-j+1)_{j-1} \sigma_{\langle k \rangle}^{i-j}. \quad (120)$$

In particular, for ${}_0\tilde{F}_0^{(n)}(\mathbf{\Lambda}, \mathbf{\Sigma})$, $K_{p,q}^{m,n}$ in (118) and the (i, j) th entry of \mathcal{Y}_k in (119) reduce to

$$K_{0,0}^{m,n} = \prod_{i=1}^m (n-i)! \quad (121)$$

$$\mathcal{Y}_{k,ij} = \lambda_i^{j-1} e^{\lambda_i \sigma_{\langle k \rangle}}. \quad (122)$$

Proof: Let us dilate the $m \times m$ matrix $\mathbf{\Lambda}$ to the $n \times n$ matrix $\mathbf{\Lambda} \oplus \mathbf{0}_{n-m}$ by affixing zero elements. Then, this augmented matrix $\mathbf{\Lambda} \oplus \mathbf{0}_{n-m}$ has the eigenvalues $\lambda_1, \lambda_2, \dots, \lambda_m$ and $(n-m)$ additional zero eigenvalues. Note that zonal polynomials depend on its Hermitian matrix arguments through Schur functions in the eigenvalues of matrix arguments [66]–[69]. Since Schur functions are invariant to augmenting zero elements [71], it is easy to show that

$$\tilde{C}_\kappa(\mathbf{\Lambda} \oplus \mathbf{0}_{n-m}) = \tilde{C}_\kappa(\mathbf{\Lambda}). \quad (123)$$

Let $\lambda_{m+1}, \lambda_{m+2}, \dots, \lambda_n$ be $(n-m)$ additional zero eigenvalues and denote the left-hand side of (117) by $\text{LHS}_{(117)}$ for convenience. Then, it follows from (123) and [68, Lemma 3] that

$$\text{LHS}_{(117)} = K_{p,q}^{n,n} \frac{\det_{1 \leq i, j \leq n} (\mathcal{H}_{p,q}^{n,1}(\lambda_i \sigma_j))}{\prod_{i < j}^n (\lambda_j - \lambda_i) (\sigma_j - \sigma_i)} \cdot \prod_{i < j}^m (\lambda_j - \lambda_i). \quad (124)$$

From a computational point of view, (124) presents numerical difficulty since the Vandermonde determinant $\prod_{i < j}^n (\lambda_j - \lambda_i)$ or $\prod_{i < j}^n (\sigma_j - \sigma_i)$ becomes zero when some of the λ_i 's or σ_i 's are equal. This can be alleviated by using Cauchy's mean value theorem (or L'Hôspital's rule):

$$\text{LHS}_{(117)} = K_{p,q}^{n,n} \lim_{\sigma \rightarrow \tilde{\sigma}} \lim_{\{\lambda_k\}_{k=m+1}^n \rightarrow 0} \frac{\det_{1 \leq i, j \leq n} (\mathcal{H}_{p,q}^{n,1}(\lambda_i \sigma_j))}{\prod_{i < j}^n (\lambda_j - \lambda_i) (\sigma_j - \sigma_i)} \cdot \prod_{i < j}^m (\lambda_j - \lambda_i) \quad (125)$$

where $\sigma \rightarrow \tilde{\sigma}$ means that

$$\begin{aligned} \{\sigma_i\}_{i=1}^{\ell_1(\mathbf{\Sigma})} &\rightarrow \sigma_{\langle 1 \rangle}, \\ \{\sigma_i\}_{i=\ell_1(\mathbf{\Sigma})+1}^{\ell_1(\mathbf{\Sigma})+\ell_2(\mathbf{\Sigma})} &\rightarrow \sigma_{\langle 2 \rangle}, \\ &\vdots \\ \{\sigma_i\}_{i=n-\ell_{\varrho(\mathbf{\Sigma})}(\mathbf{\Sigma})+1}^n &\rightarrow \sigma_{\langle \varrho(\mathbf{\Sigma}) \rangle}. \end{aligned}$$

Let n -dimensional vectors $\mathbf{u}(z)$ and $\mathbf{v}(z)$ be

$$\mathbf{u}(z) = (\mathcal{H}_{p,q}^{n,1}(\sigma_1 z), \mathcal{H}_{p,q}^{n,1}(\sigma_2 z), \dots, \mathcal{H}_{p,q}^{n,1}(\sigma_n z)) \quad (126)$$

$$\mathbf{v}(z) = (1, z, \dots, z^{n-1}) \quad (127)$$

and let $\mathbf{u}^{(k)}(z)$ and $\mathbf{v}^{(k)}(z)$ be the k th derivatives of $\mathbf{u}(z)$ and $\mathbf{v}(z)$ with respect to z , respectively. Note that the j th components $u_j^{(k)}(z)$ and $v_j^{(k)}(z)$, $j = 1, 2, \dots, n$, of $\mathbf{u}^{(k)}(z)$ and $\mathbf{v}^{(k)}(z)$ are given respectively by

$$u_j^{(k)}(z) = \frac{\sigma_j^k}{\chi_{p,q}^{n,k}} \cdot \mathcal{H}_{p,q}^{n,k+1}(\sigma_j z) \quad (128)$$

$$v_j^{(k)}(z) = (j-k)_k z^{j-k-1} \quad (129)$$

where (128) follows from the differentiation identity of [72, eq. (7.2.3.47)]. Then, taking the limits on λ_k 's, we get

$$\lim_{\{\lambda_k\}_{k=m+1}^n \rightarrow 0} \frac{\det_{1 \leq i, j \leq n} (\mathcal{H}_{p,q}^{n,1}(\lambda_i \sigma_j))}{\prod_{i < j}^n (\lambda_j - \lambda_i)} = \frac{\det \begin{bmatrix} \mathbf{U}_A \\ \mathbf{U}_B \end{bmatrix}}{\det \begin{bmatrix} \mathbf{V}_A \\ \mathbf{V}_B \end{bmatrix}} \quad (130)$$

with the $(n-m) \times n$ matrices

$$\mathbf{U}_A = (U_{A,ij}) = \begin{bmatrix} \mathbf{u}^{(0)}(0) \\ \mathbf{u}^{(1)}(0) \\ \vdots \\ \mathbf{u}^{(n-m-1)}(0) \end{bmatrix} \quad (131)$$

$$\mathbf{V}_A = (V_{A,ij}) = \begin{bmatrix} \mathbf{v}^{(0)}(0) \\ \mathbf{v}^{(1)}(0) \\ \vdots \\ \mathbf{v}^{(n-m-1)}(0) \end{bmatrix}, \quad (132)$$

and the $m \times n$ matrices $\mathbf{U}_B = (\mathcal{H}_{p,q}^{n,1}(\lambda_i \sigma_j))$ and $\mathbf{V}_B = (\lambda_i^{j-1})$. From (128) and (129), it is easy to see that the (i, j) th entries of \mathbf{U}_A and \mathbf{V}_A are given respectively by

$$U_{A,ij} = u_j^{(i-1)}(0) = \frac{\sigma_j^{i-1}}{\chi_{p,q}^{n,i-1}} \quad (133)$$

$$V_{A,ij} = v_j^{(i-1)}(0) = \begin{cases} (i-1)!, & \text{if } i = j \\ 0, & \text{otherwise.} \end{cases} \quad (134)$$

Now, using the result on the determinant of a partitioned matrix

$$\det \left(\begin{bmatrix} \mathbf{A} & \mathbf{B} \\ \mathbf{C} & \mathbf{D} \end{bmatrix} \right) = \det(\mathbf{A}) \det(\mathbf{D} - \mathbf{C}\mathbf{A}^{-1}\mathbf{B}), \quad \text{if } \mathbf{A} \text{ is invertible,} \quad (135)$$

we have

$$\begin{aligned} \det \left(\begin{bmatrix} \mathbf{V}_A \\ \mathbf{V}_B \end{bmatrix} \right) &= \prod_{l=1}^{n-m} (l-1)! \cdot \det \left(\begin{bmatrix} \lambda_1^{n-m} & \lambda_1^{n-m+1} & \cdots & \lambda_1^{n-1} \\ \lambda_2^{n-m} & \lambda_2^{n-m+1} & \cdots & \lambda_2^{n-1} \\ \vdots & \vdots & \ddots & \vdots \\ \lambda_m^{n-m} & \lambda_m^{n-m+1} & \cdots & \lambda_m^{n-1} \end{bmatrix} \right) \\ &= \prod_{l=1}^{n-m} (l-1)! \prod_{k=1}^m \lambda_k^{n-m} \prod_{i < j}^m (\lambda_j - \lambda_i). \end{aligned} \quad (136)$$

Hence, combining (125), (130), and (136) gives

$$\text{LHS}_{(117)} = \frac{K_{p,q}^{m,n}}{\det(\mathbf{\Lambda})^{n-m}} \lim_{\boldsymbol{\sigma} \rightarrow \tilde{\boldsymbol{\sigma}}} \frac{\det \left(\begin{bmatrix} \tilde{\mathbf{U}}_A \\ \mathbf{U}_B \end{bmatrix} \right)}{\prod_{i < j}^n (\sigma_j - \sigma_i)} \quad (137)$$

where $\tilde{\mathbf{U}}_A = (\sigma_j^{i-1})$ is the $(n-m) \times n$ submatrix of the Vandermonde matrix of $\sigma_1, \sigma_2, \dots, \sigma_n$.

Using similar steps leading to (130), we obtain

$$\lim_{\boldsymbol{\sigma} \rightarrow \tilde{\boldsymbol{\sigma}}} \frac{\det \left(\begin{bmatrix} \tilde{\mathbf{U}}_A \\ \mathbf{U}_B \end{bmatrix} \right)}{\prod_{i < j}^n (\sigma_j - \sigma_i)} = \frac{\det \left(\begin{bmatrix} \mathbf{Z}_{(n-m),1} & \mathbf{Z}_{(n-m),2} & \cdots & \mathbf{Z}_{(n-m),\varrho(\boldsymbol{\Sigma})} \\ \mathbf{Y}_1 & \mathbf{Y}_2 & \cdots & \mathbf{Y}_{\varrho(\boldsymbol{\Sigma})} \end{bmatrix} \right)}{\det \left(\begin{bmatrix} \mathbf{Z}_{(n),1} & \mathbf{Z}_{(n),2} & \cdots & \mathbf{Z}_{(n),\varrho(\boldsymbol{\Sigma})} \end{bmatrix} \right)} \quad (138)$$

where the (i, j) th entries of $m \times \ell_k(\boldsymbol{\Sigma})$ matrices \mathbf{Y}_k and $l \times \ell_k(\boldsymbol{\Sigma})$ matrices $\mathbf{Z}_{(l),k}$, $l \leq n$, $k = 1, 2, \dots, \varrho(\boldsymbol{\Sigma})$, are given by (119) and (120), respectively. Finally, substituting (138) into (137) completes the proof of the lemma. \square

As a by-product of Lemma 4, we obtain the following determinantal formula for the hypergeometric function of one matrix argument.

Corollary 5: If $\boldsymbol{\Sigma} = \mathbf{I}_n$ in Lemma 4, then we have

$${}_p\tilde{F}_q(a_1, \dots, a_p; b_1, \dots, b_q; \mathbf{\Lambda}) \cdot \prod_{i < j}^m (\lambda_j - \lambda_i) = \det_{1 \leq i, j \leq m} (\lambda_i^{j-1} \mathcal{H}_{p,q}^{n, n-m+j}(\lambda_i)). \quad (139)$$

Proof: The result follows immediately from (135) and Lemma 4 with $\varrho(\boldsymbol{\Sigma}) = 1$, $\ell_1(\boldsymbol{\Sigma}) = n$, and $\sigma_{\langle 1 \rangle} = 1$. \square

C. Some Statistics Derived from Complex Gaussian Matrices

Lemma 5: Let $\mathbf{X} \sim \tilde{\mathcal{N}}_{m,n}(\mathbf{0}_{m \times n}, \mathbf{\Sigma}, \mathbf{\Psi})$. Then, for $\mathbf{A} \in \mathbb{C}^{m \times m} \geq 0$ and $\mathbf{B} \in \mathbb{C}^{n \times n} \geq 0$, the k th-order cumulant of $\text{tr}(\mathbf{A}\mathbf{X}\mathbf{B}\mathbf{X}^\dagger)$ is

$$\begin{aligned} \text{Cum}_k \left\{ \text{tr}(\mathbf{A}\mathbf{X}\mathbf{B}\mathbf{X}^\dagger) \right\} &\triangleq (-1)^k \left. \frac{d^k}{ds^k} \ln \phi_{\text{tr}(\mathbf{A}\mathbf{X}\mathbf{B}\mathbf{X}^\dagger)}(s) \right|_{s=0} \\ &= (k-1)! \text{tr}\{(\mathbf{A}\mathbf{\Sigma})^k\} \text{tr}\{(\mathbf{\Psi}\mathbf{B})^k\} \end{aligned} \quad (140)$$

where $\phi_{\text{tr}(\mathbf{A}\mathbf{X}\mathbf{B}\mathbf{X}^\dagger)}(s) \triangleq \mathbb{E}\{\text{etr}(-s\mathbf{A}\mathbf{X}\mathbf{B}\mathbf{X}^\dagger)\}$ is the MGF of $\text{tr}(\mathbf{A}\mathbf{X}\mathbf{B}\mathbf{X}^\dagger)$.

Proof: Since

$$\text{tr}(\mathbf{A}\mathbf{X}\mathbf{B}\mathbf{X}^\dagger) = (\text{vec}(\mathbf{X}^\dagger))^\dagger (\mathbf{A}^T \otimes \mathbf{B}) \text{vec}(\mathbf{X}^\dagger)$$

is a quadratic form in complex Gaussian variables, whose characteristic function has been reported in [73], it can be readily shown that

$$\begin{aligned} \phi_{\text{tr}(\mathbf{A}\mathbf{X}\mathbf{B}\mathbf{X}^\dagger)}(s) &= \det \left\{ \mathbf{I}_{mn} + s(\mathbf{\Sigma}^T \otimes \mathbf{\Psi})(\mathbf{A}^T \otimes \mathbf{B}) \right\}^{-1} \\ &= \det(\mathbf{I}_{mn} + s\mathbf{A}\mathbf{\Sigma} \otimes \mathbf{\Psi}\mathbf{B})^{-1}. \end{aligned} \quad (141)$$

Therefore,

$$\frac{d^k}{ds^k} \ln \phi_{\text{tr}(\mathbf{A}\mathbf{X}\mathbf{B}\mathbf{X}^\dagger)}(s) = (-1)^k (k-1)! \text{tr} \left\{ \left[(\mathbf{I}_{mn} + s\mathbf{A}\mathbf{\Sigma} \otimes \mathbf{\Psi}\mathbf{B})^{-1} (\mathbf{A}\mathbf{\Sigma} \otimes \mathbf{\Psi}\mathbf{B}) \right]^k \right\}. \quad (142)$$

Hence, we obtain the result (140) from the properties (94), (96), and (142) with $s = 0$. \square

We remark that the cumulants, except for the first-order cumulant, are invariant with respect to translations of a random variable. The first and second order cumulants are the mean and variance of the underlying random variable, respectively, and other higher-order statistics can also be obtained from general relationships between the cumulants and moments [74, Table 2.2]. Lemma 5 reveals that all cumulants of $\text{tr}(\mathbf{A}\mathbf{X}\mathbf{B}\mathbf{X}^\dagger)$ as functionals of the eigenvalues of $\mathbf{A}\mathbf{\Sigma}$ and $\mathbf{\Psi}\mathbf{B}$ are MIS.

Lemma 6: Let $\mathbf{X} \sim \tilde{\mathcal{N}}_{m,n}(\mathbf{0}_{m \times n}, \mathbf{\Sigma}, \mathbf{\Psi})$. Then, for $\mathbf{A} \in \mathbb{C}^{m \times m} \geq 0$ and $\mathbf{B} \in \mathbb{C}^{n \times n} \geq 0$, we have

$$\mathbb{E} \left\{ \text{tr} \left[(\mathbf{A}\mathbf{X}\mathbf{B}\mathbf{X}^\dagger)^2 \right] \right\} = \text{tr}^2(\mathbf{A}\mathbf{\Sigma}) \text{tr}\{(\mathbf{\Psi}\mathbf{B})^2\} + \text{tr}^2(\mathbf{\Psi}\mathbf{B}) \text{tr}\{(\mathbf{A}\mathbf{\Sigma})^2\}. \quad (143)$$

Proof: We first start with the characteristic function of $\mathbf{S} = (S_{ij}) = \mathbf{A}^{1/2} \mathbf{X} \mathbf{B}^{1/2}$. Let $\tilde{\Sigma} = (\tilde{\Sigma}_{ij}) = \mathbf{A}^{1/2} \Sigma \mathbf{A}^{1/2}$ and $\tilde{\Psi} = (\tilde{\Psi}_{ij}) = \mathbf{B}^{1/2} \Psi \mathbf{B}^{1/2}$. Then,

$$\begin{aligned} \Phi_{\mathbf{S}}(\mathbf{Z}) &= \mathbb{E} \left\{ \exp \left[j \Re \operatorname{tr}(\mathbf{A}^{1/2} \mathbf{X} \mathbf{B}^{1/2} \mathbf{Z}^\dagger) \right] \right\} \\ &= \Phi_{\mathbf{X}} \left(\mathbf{A}^{1/2} \mathbf{Z} \mathbf{B}^{1/2} \right) \\ &\stackrel{(a)}{=} \operatorname{etr} \left(-\frac{1}{4} \tilde{\Sigma} \mathbf{Z} \tilde{\Psi} \mathbf{Z}^\dagger \right) \\ &= e^{\varphi(\mathbf{Z})} \end{aligned} \tag{144}$$

where (a) follows from Lemma 3 and

$$\varphi(\mathbf{Z}) = -\frac{1}{4} \sum_{i=1}^m \sum_{p=1}^m \sum_{q=1}^n \sum_{j=1}^n \tilde{\Sigma}_{ip} Z_{pj} \tilde{\Psi}_{jq} Z_{iq}^*. \tag{145}$$

It follows from the characteristic function $\Phi_{\mathbf{S}}(\mathbf{Z})$ in (144) that

$$\begin{aligned} \mathbb{E} \{ S_{i_1 j_1} S_{i_2 j_2}^* S_{i_3 j_3} S_{i_4 j_4}^* \} &= \frac{1}{j^4} \frac{\partial \Phi_{\mathbf{S}}(\mathbf{Z})}{\partial Z_{i_1 j_1} \partial Z_{i_2 j_2}^* \partial Z_{i_3 j_3} \partial Z_{i_4 j_4}^*} \Big|_{\mathbf{Z}=\mathbf{0}} \\ &= \frac{1}{j^4} \left[\frac{\partial \varphi_3(\mathbf{Z})}{\partial \Re Z_{i_4 j_4}} - j \frac{\partial \varphi_3(\mathbf{Z})}{\partial \Im Z_{i_4 j_4}} \right] \Big|_{\mathbf{Z}=\mathbf{0}} \\ &= \tilde{\Sigma}_{i_1 i_2} \tilde{\Psi}_{j_1 j_2}^* \tilde{\Sigma}_{i_3 i_4} \tilde{\Psi}_{j_3 j_4}^* + \tilde{\Sigma}_{i_1 i_4} \tilde{\Psi}_{j_1 j_4}^* \tilde{\Sigma}_{i_3 i_2} \tilde{\Psi}_{j_3 j_2}^* \end{aligned} \tag{146}$$

with

$$\varphi_1(\mathbf{Z}) = e^{\varphi(\mathbf{Z})} \left[\frac{\partial \varphi(\mathbf{Z})}{\partial \Re Z_{i_1 j_1}} + j \frac{\partial \varphi(\mathbf{Z})}{\partial \Im Z_{i_1 j_1}} \right] \tag{147}$$

$$\varphi_2(\mathbf{Z}) = \frac{\partial \varphi_1(\mathbf{Z})}{\partial \Re Z_{i_2 j_2}} - j \frac{\partial \varphi_1(\mathbf{Z})}{\partial \Im Z_{i_2 j_2}} \tag{148}$$

$$\varphi_3(\mathbf{Z}) = \frac{\partial \varphi_2(\mathbf{Z})}{\partial \Re Z_{i_3 j_3}} + j \frac{\partial \varphi_2(\mathbf{Z})}{\partial \Im Z_{i_3 j_3}}. \tag{149}$$

Using (146), we obtain

$$\begin{aligned}
\mathbb{E}_{\mathbf{X}} \left\{ \text{tr} \left[(\mathbf{A} \mathbf{X} \mathbf{B} \mathbf{X}^\dagger)^2 \right] \right\} &= \mathbb{E}_{\mathbf{S}} \left\{ \text{tr} \left[(\mathbf{S} \mathbf{S}^\dagger)^2 \right] \right\} \\
&= \sum_{i=1}^m \sum_{p=1}^n \sum_{q=1}^n \sum_{j=1}^m \mathbb{E} \{ S_{ip} S_{jp}^* S_{jq} S_{iq}^* \} \\
&= \sum_{i=1}^m \sum_{p=1}^n \sum_{q=1}^n \sum_{j=1}^m \left(\tilde{\Sigma}_{ij} \tilde{\Psi}_{pp} \tilde{\Sigma}_{ji} \tilde{\Psi}_{qq} + \tilde{\Sigma}_{ii} \tilde{\Psi}_{pq} \tilde{\Sigma}_{jj} \tilde{\Psi}_{qp} \right) \\
&= \text{tr}^2(\tilde{\Sigma}) \text{tr}(\tilde{\Psi}^2) + \text{tr}^2(\tilde{\Psi}) \text{tr}(\tilde{\Sigma}^2)
\end{aligned} \tag{150}$$

from which (143) follows readily. \square

Theorem 7: Let $\mathbf{X}_1 \sim \tilde{\mathcal{N}}_{m,p}(\mathbf{0}_{m \times p}, \mathbf{\Sigma}_1, \mathbf{\Psi}_1)$ and $\mathbf{X}_2 \sim \tilde{\mathcal{N}}_{p,n}(\mathbf{0}_{p \times n}, \mathbf{\Sigma}_2, \mathbf{\Psi}_2)$ be statistically independent complex Gaussian matrices. Then,

$$\begin{aligned}
&\mathbb{E}_{\mathbf{X}_1, \mathbf{X}_2} \left\{ \text{tr}^2(\mathbf{X}_1 \mathbf{X}_2 \mathbf{X}_2^\dagger \mathbf{X}_1^\dagger) \right\} \\
&= \text{tr}(\mathbf{\Sigma}_1^2) \text{tr}^2(\mathbf{\Psi}_1 \mathbf{\Sigma}_2) \text{tr}(\mathbf{\Psi}_2^2) + \text{tr}(\mathbf{\Sigma}_1^2) \text{tr}^2(\mathbf{\Psi}_2) \text{tr}\{(\mathbf{\Psi}_1 \mathbf{\Sigma}_2)^2\} \\
&\quad + \text{tr}^2(\mathbf{\Sigma}_1) \text{tr}\{(\mathbf{\Psi}_1 \mathbf{\Sigma}_2)^2\} \text{tr}(\mathbf{\Psi}_2^2) + \text{tr}^2(\mathbf{\Sigma}_1) \text{tr}^2(\mathbf{\Psi}_1 \mathbf{\Sigma}_2) \text{tr}^2(\mathbf{\Psi}_2)
\end{aligned} \tag{151}$$

and

$$\begin{aligned}
&\mathbb{E}_{\mathbf{X}_1, \mathbf{X}_2} \left\{ \text{tr} \left[(\mathbf{X}_1 \mathbf{X}_2 \mathbf{X}_2^\dagger \mathbf{X}_1^\dagger)^2 \right] \right\} \\
&= \text{tr}^2(\mathbf{\Sigma}_1) \text{tr}^2(\mathbf{\Psi}_1 \mathbf{\Sigma}_2) \text{tr}(\mathbf{\Psi}_2^2) + \text{tr}^2(\mathbf{\Sigma}_1) \text{tr}^2(\mathbf{\Psi}_2) \text{tr}\{(\mathbf{\Psi}_1 \mathbf{\Sigma}_2)^2\} \\
&\quad + \text{tr}\{(\mathbf{\Psi}_1 \mathbf{\Sigma}_2)^2\} \text{tr}(\mathbf{\Psi}_2^2) \text{tr}(\mathbf{\Sigma}_1^2) + \text{tr}^2(\mathbf{\Psi}_1 \mathbf{\Sigma}_2) \text{tr}^2(\mathbf{\Psi}_2) \text{tr}(\mathbf{\Sigma}_1^2).
\end{aligned} \tag{152}$$

Proof: Using the first two cumulants from Lemma 5, we get

$$\begin{aligned}
&\mathbb{E}_{\mathbf{X}_1, \mathbf{X}_2} \left\{ \text{tr}^2(\mathbf{X}_1 \mathbf{X}_2 \mathbf{X}_2^\dagger \mathbf{X}_1^\dagger) \right\} \\
&= \mathbb{E}_{\mathbf{X}_2} \left\{ \text{tr}(\mathbf{\Sigma}_1^2) \text{tr} \left[(\mathbf{X}_2 \mathbf{X}_2^\dagger \mathbf{\Psi}_1)^2 \right] + \text{tr}^2(\mathbf{\Sigma}_1) \text{tr}^2(\mathbf{X}_2 \mathbf{X}_2^\dagger \mathbf{\Psi}_1) \right\}
\end{aligned} \tag{153}$$

where it follows from Lemma 6 that

$$\mathbb{E}_{\mathbf{X}_2} \left\{ \text{tr} \left[(\mathbf{X}_2 \mathbf{X}_2^\dagger \mathbf{\Psi}_1)^2 \right] \right\} = \text{tr}^2(\mathbf{\Psi}_1 \mathbf{\Sigma}_2) \text{tr}(\mathbf{\Psi}_2^2) + \text{tr}^2(\mathbf{\Psi}_2) \text{tr}\{(\mathbf{\Psi}_1 \mathbf{\Sigma}_2)^2\} \tag{154}$$

and from Lemma 5 that

$$\mathbb{E}_{\mathbf{X}_2} \left\{ \text{tr}^2(\mathbf{X}_2 \mathbf{X}_2^\dagger \boldsymbol{\Psi}_1) \right\} = \text{tr} \{ (\boldsymbol{\Psi}_1 \boldsymbol{\Sigma}_2)^2 \} \text{tr}(\boldsymbol{\Psi}_2^2) + \text{tr}^2(\boldsymbol{\Psi}_1 \boldsymbol{\Sigma}_2) \text{tr}^2(\boldsymbol{\Psi}_2). \quad (155)$$

Combining (153)–(155) yields the desired result (151).

Similar to (153), we have

$$\begin{aligned} & \mathbb{E}_{\mathbf{X}_1, \mathbf{X}_2} \left\{ \text{tr} \left[(\mathbf{X}_1 \mathbf{X}_2 \mathbf{X}_2^\dagger \mathbf{X}_1^\dagger)^2 \right] \right\} \\ &= \mathbb{E}_{\mathbf{X}_2} \left\{ \text{tr}^2(\boldsymbol{\Sigma}_1) \text{tr} \left[(\mathbf{X}_2 \mathbf{X}_2^\dagger \boldsymbol{\Psi}_1)^2 \right] + \text{tr}^2(\mathbf{X}_2 \mathbf{X}_2^\dagger \boldsymbol{\Psi}_1) \text{tr}(\boldsymbol{\Sigma}_1^2) \right\}. \end{aligned} \quad (156)$$

From (154)–(156), we obtain the desired result (152). \square

Theorem 8: Let $\mathbf{X} \sim \tilde{\mathcal{N}}_{m,n}(\mathbf{0}_{m \times n}, \boldsymbol{\Sigma}, \mathbf{I}_n)$, $m \leq n$, and $\sigma_1, \sigma_2, \dots, \sigma_m$ be the eigenvalues of $\boldsymbol{\Sigma}$ in any order. Then, the joint pdf of the ordered eigenvalues $\lambda_1 \geq \lambda_2 \geq \dots \geq \lambda_m > 0$ of a central complex Wishart matrix $\mathbf{X} \mathbf{X}^\dagger \sim \tilde{\mathcal{W}}_m(n, \boldsymbol{\Sigma})$ is given by

$$p_{\boldsymbol{\lambda}}(\lambda_1, \lambda_2, \dots, \lambda_m) = \mathcal{A}^{-1} \det \left([\mathbf{G}_1 \quad \mathbf{G}_2 \quad \dots \quad \mathbf{G}_{\varrho(\boldsymbol{\Sigma})}] \right) \det_{1 \leq i, j \leq m} (\lambda_j^{i-1}) \prod_{k=1}^m \lambda_k^{n-m} \quad (157)$$

where

$$\mathcal{A} = K_{0,0}^{m,n} \cdot \det \left([\mathbf{B}_1 \quad \mathbf{B}_2 \quad \dots \quad \mathbf{B}_{\varrho(\boldsymbol{\Sigma})}] \right) \quad (158)$$

and $\mathbf{G}_k = (G_{k,ij})$ and $\mathbf{B}_k = (\mathcal{B}_{k,ij})$, $k = 1, 2, \dots, \varrho(\boldsymbol{\Sigma})$, are $m \times \ell_k(\boldsymbol{\Sigma})$ matrices, whose (i, j) th entries are given respectively by

$$G_{k,ij} = \lambda_i^{j-1} e^{-\lambda_i / \sigma_{\langle k \rangle}} \quad (159)$$

$$\mathcal{B}_{k,ij} = (-1)^{i-j} (i - j + 1)_{j-1} \sigma_{\langle k \rangle}^{n-i+j}. \quad (160)$$

Proof: The joint eigenvalue density $p_{\boldsymbol{\lambda}}(\lambda_1, \lambda_2, \dots, \lambda_m)$ is given in terms of the hypergeometric function of matrix arguments as follows [66]:

$$p_{\boldsymbol{\lambda}}(\lambda_1, \lambda_2, \dots, \lambda_m) = \frac{\pi^{m(m-1)} \det(\boldsymbol{\Sigma})^{-n}}{\tilde{\Gamma}_m(n) \tilde{\Gamma}_m(m)} {}_0\tilde{F}_0^{(m)}(\mathbf{D}, -\boldsymbol{\Sigma}^{-1}) \prod_{k=1}^m \lambda_k^{n-m} \prod_{i < j}^m (\lambda_i - \lambda_j)^2 \quad (161)$$

where $\mathbf{D} = \text{diag}(\lambda_1, \lambda_2, \dots, \lambda_m)$. To render the joint pdf more amenable to further analysis and computationally tractable, we apply Lemma 4 to (161), which results in (157) after some algebra. \square

Note that (157) is valid for any covariance matrix $\mathbf{\Sigma}$ with the eigenvalues of arbitrary multiplicity and hence, generalizes the previous determinantal representation for the joint eigenvalue pdf of Wishart matrices. If $\mathbf{\Sigma} = \mathbf{I}_m$ in Theorem 8, all of the eigenvalues are identically equal to one and hence, with $\varrho(\mathbf{\Sigma}) = 1$, $\ell_1(\mathbf{\Sigma}) = m$, and $\sigma_{\langle 1 \rangle} = 1$, (157) reduces to [29, eq. (6)]. Furthermore, if all the eigenvalues of $\mathbf{\Sigma}$ are distinct, then, with $\varrho(\mathbf{\Sigma}) = m$ and $\ell_1(\mathbf{\Sigma}) = \ell_2(\mathbf{\Sigma}) = \dots = \ell_m(\mathbf{\Sigma}) = 1$, (157) reduces to [29, eq. (18)].

Theorem 9: Let $\mathbf{X} \sim \tilde{\mathcal{N}}_{m,n}(\mathbf{0}_{m \times n}, \mathbf{I}_m, \mathbf{\Psi})$, $m \leq n$, $\mathbf{A} \in \mathbb{C}^{n \times n}$ be Hermitian positive definite, and $\beta_1, \beta_2, \dots, \beta_n$ be the eigenvalues of $\mathbf{A}^{1/2} \mathbf{\Psi} \mathbf{A}^{1/2}$ in any order. Then, the joint pdf of the ordered eigenvalues $\lambda_1 \geq \lambda_2 \geq \dots \geq \lambda_m > 0$ of a matrix quadratic form $\mathbf{X} \mathbf{A} \mathbf{X}^\dagger$ is given by

$$p_{\lambda}(\lambda_1, \lambda_2, \dots, \lambda_m) = \frac{\det \left(\begin{bmatrix} \mathbf{V}_{(n-m),1} & \mathbf{V}_{(n-m),2} & \cdots & \mathbf{V}_{(n-m),\varrho(\mathbf{A}^{1/2} \mathbf{\Psi} \mathbf{A}^{1/2})} \\ \mathbf{Q}_1 & \mathbf{Q}_2 & \cdots & \mathbf{Q}_{\varrho(\mathbf{A}^{1/2} \mathbf{\Psi} \mathbf{A}^{1/2})} \end{bmatrix} \right)}{K_{0,0}^{m,m} \det(\mathbf{A} \mathbf{\Psi})^m \det \left(\begin{bmatrix} \mathbf{V}_{(n),1} & \mathbf{V}_{(n),2} & \cdots & \mathbf{V}_{(n),\varrho(\mathbf{A}^{1/2} \mathbf{\Psi} \mathbf{A}^{1/2})} \end{bmatrix} \right)} \prod_{1 \leq i, j \leq m} (\lambda_j^{i-1}) \quad (162)$$

where $\mathbf{Q}_k = (Q_{k,ij})$ and $\mathbf{V}_{(l),k} = (\mathcal{V}_{(l),k,ij})$, $l \leq n$, $k = 1, 2, \dots, \varrho(\mathbf{A}^{1/2} \mathbf{\Psi} \mathbf{A}^{1/2})$, are $m \times \ell_k(\mathbf{A}^{1/2} \mathbf{\Psi} \mathbf{A}^{1/2})$ and $l \times \ell_k(\mathbf{A}^{1/2} \mathbf{\Psi} \mathbf{A}^{1/2})$ matrices, whose (i, j) th entries are given respectively by

$$Q_{k,ij} = \lambda_i^{j-1} e^{-\lambda_i / \beta_{\langle k \rangle}} \quad (163)$$

$$\mathcal{V}_{(l),k,ij} = (-1)^{i-j} (i - j + 1)_{j-1} \beta_{\langle k \rangle}^{-i+j}. \quad (164)$$

Proof: Let $\mathbf{S} = \mathbf{X} \mathbf{A} \mathbf{X}^\dagger$, then $\mathbf{S} \sim \tilde{\mathcal{Q}}_{m,n}(\mathbf{A}, \mathbf{I}_m, \mathbf{\Psi})$ is a positive-definite quadratic form in the complex Gaussian matrix [28, Definition II.3], whose pdf is given by [30]

$$p_{\mathbf{S}}(\mathbf{S}) = \frac{1}{\tilde{\Gamma}_m(n)} \det(\mathbf{A} \mathbf{\Psi})^{-m} \det(\mathbf{S})^{n-m} {}_0\tilde{F}_0^{(n)}(-\mathbf{S}, \mathbf{\Psi}^{-1} \mathbf{A}^{-1}), \quad \mathbf{S} > 0. \quad (165)$$

Using (165), we can write the joint eigenvalue pdf of \mathbf{S} in the form

$$\begin{aligned} p_{\lambda}(\lambda_1, \lambda_2, \dots, \lambda_m) &= \frac{\pi^{m(m-1)}}{\tilde{\Gamma}_m(m)} \int_{\mathbf{U} \in \mathcal{U}(m)} p_{\mathbf{S}}(\mathbf{U} \mathbf{D} \mathbf{U}^\dagger) \prod_{i < j}^m (\lambda_i - \lambda_j)^2 [d\mathbf{U}] \\ &= \frac{\pi^{m(m-1)} \det(\mathbf{A} \mathbf{\Psi})^{-m}}{\tilde{\Gamma}_m(n) \tilde{\Gamma}_m(m)} {}_0\tilde{F}_0^{(n)}(\mathbf{D}, -\mathbf{\Psi}^{-1} \mathbf{A}^{-1}) \prod_{k=1}^m \lambda_k^{n-m} \prod_{i < j}^m (\lambda_i - \lambda_j)^2 \end{aligned} \quad (166)$$

where $\mathbf{D} = \text{diag}(\lambda_1, \lambda_2, \dots, \lambda_m)$, $\mathcal{U}(m) = \{\mathbf{U} : \mathbf{U} \mathbf{U}^\dagger = \mathbf{I}_m\}$ is the unitary group of order m , and $[d\mathbf{U}]$ is the unitary invariant Haar measure on the unitary group $\mathcal{U}(m)$ normalized to make the total volume unity. Similar to Theorem 8, we obtain the desired result (162) applying Lemma 4 to (166). \square

Definition 6 (Characteristic Coefficient): Let \mathbf{A} be an $n \times n$ Hermitian matrix with the eigenvalues $\alpha_1, \alpha_2, \dots, \alpha_n$ in any order. Then, the (i, j) th characteristic coefficient $\mathcal{X}_{i,j}(\mathbf{A})$, $i = 1, 2, \dots, \varrho(\mathbf{A})$, $j = 1, 2, \dots, \ell_i(\mathbf{A})$, is defined as a partial fraction expansion coefficient of $\det(\mathbf{I}_n + \xi \mathbf{A})^{-1}$ such that

$$\begin{aligned} \det(\mathbf{I}_n + \xi \mathbf{A})^{-1} &= \prod_{i=1}^{\varrho(\mathbf{A})} (1 + \xi \alpha_{\langle i \rangle})^{-\ell_i(\mathbf{A})} \\ &= \sum_{i=1}^{\varrho(\mathbf{A})} \sum_{j=1}^{\ell_i(\mathbf{A})} \mathcal{X}_{i,j}(\mathbf{A}) (1 + \xi \alpha_{\langle i \rangle})^{-j} \end{aligned} \quad (167)$$

where ξ is a scalar constant such that $\mathbf{I}_n + \xi \mathbf{A}$ is nonsingular. The (i, j) th characteristic coefficient $\mathcal{X}_{i,j}(\mathbf{A})$ can be determined by

$$\begin{aligned} \mathcal{X}_{i,j}(\mathbf{A}) &= \frac{1}{\varpi_{i,j}! \alpha_{\langle i \rangle}^{\varpi_{i,j}}} \cdot \left[\frac{d^{\varpi_{i,j}}}{dv^{\varpi_{i,j}}} (1 + v \alpha_{\langle i \rangle})^{\ell_i(\mathbf{A})} \det(\mathbf{I}_n + v \mathbf{A})^{-1} \right] \Big|_{v=-1/\alpha_{\langle i \rangle}} \\ &= \frac{1}{\varpi_{i,j}! \alpha_{\langle i \rangle}^{\varpi_{i,j}}} \sum_{\substack{k_1+k_2+\dots+k_{\varrho(\mathbf{A})}=\varpi_{i,j} \\ k_l \in \{0, \mathbb{N}\} \text{ for } \forall l \neq i \\ k_i=0}} \frac{\varpi_{i,j}!}{k_1! k_2! \dots k_{\varrho(\mathbf{A})}!} \prod_{\substack{l=1 \\ l \neq i}}^{\varrho(\mathbf{A})} \left[\frac{d^{k_l}}{dv^{k_l}} (1 + v \alpha_{\langle l \rangle})^{-\ell_l(\mathbf{A})} \right] \Big|_{v=-1/\alpha_{\langle i \rangle}} \\ &= \frac{(-1)^{\varpi_{i,j}}}{\alpha_{\langle i \rangle}^{\varpi_{i,j}}} \sum_{\substack{k_1+k_2+\dots+k_{\varrho(\mathbf{A})}=\varpi_{i,j} \\ k_l \in \{0, \mathbb{N}\} \text{ for } \forall l \neq i \\ k_i=0}} \prod_{\substack{l=1 \\ l \neq i}}^{\varrho(\mathbf{A})} \binom{\ell_l(\mathbf{A}) + k_l - 1}{k_l} \frac{\alpha_{\langle l \rangle}^{k_l}}{\left(1 - \frac{\alpha_{\langle l \rangle}}{\alpha_{\langle i \rangle}}\right)^{\ell_l(\mathbf{A}) + k_l}} \end{aligned} \quad (168)$$

where $\varpi_{i,j} = \ell_p(\mathbf{A}) - q$ and the second equality can be obtained using the classical rule for the derivative of determinants [75].

Note that the characteristic coefficients are invariant with respect to the constant ξ and only a function of the spectra of \mathbf{A} . In addition, it can be seen from (167) with $\xi = 0$ that the sum of all the characteristic coefficients is equal to one. By definition, we have

$$\mathcal{X}_{1,j}(\mathbf{I}_n) = \begin{cases} 0, & j = 1, 2, \dots, n-1 \\ 1, & j = n. \end{cases} \quad (169)$$

Example 6 (Constant Correlation Matrix): Consider a constant correlation matrix $\Phi_n^{(c)}(\rho)$. Since the eigenvalues of $\Phi_n^{(c)}(\rho)$ are $1 + (n-1)\rho$ and $1 - \rho$ with $n-1$ multiplicity, it is easy to show that the characteristic coefficients of $\Phi_n^{(c)}(\rho)$, $\rho \in (0, 1)$, are

$$\mathcal{X}_{1,1}(\Phi_n^{(c)}(\rho)) = \left(\frac{n\rho}{1 - \rho + n\rho} \right)^{-n+1} \quad (170)$$

$$\mathcal{X}_{2,j}(\Phi_n^{(c)}(\rho)) = -\frac{1 - \rho}{1 - \rho + n\rho} \cdot \left(\frac{n\rho}{1 - \rho + n\rho} \right)^{-n+j} \quad (171)$$

where $j = 1, 2, \dots, n-1$.

Theorem 10: Let $\mathbf{X} \sim \tilde{\mathcal{N}}_{m,n}(\mathbf{0}_{m \times n}, \mathbf{\Sigma}, \mathbf{I}_n)$, $m \leq n$, and $\sigma_1, \sigma_2, \dots, \sigma_m$ be the eigenvalues of $\mathbf{\Sigma}$. Let \mathbf{A} be a $\nu \times \nu$ positive-semidefinite matrix with the eigenvalues $\alpha_1, \alpha_2, \dots, \alpha_\nu$. Then, for $\xi \geq 0$, we have

$$\mathbb{E} \left\{ \det(\mathbf{I}_{m\nu} + \xi \mathbf{A} \otimes \mathbf{X} \mathbf{X}^\dagger)^{-1} \right\} = \mathcal{A}^{-1} \det([\mathbf{\Omega}_1 \quad \mathbf{\Omega}_2 \quad \dots \quad \mathbf{\Omega}_{\varrho(\mathbf{\Sigma})}]) \quad (172)$$

where \mathcal{A} is given in (158) and $\mathbf{\Omega}_k = (\Omega_{k,ij})$, $k = 1, 2, \dots, \varrho(\mathbf{\Sigma})$, are $m \times \ell_k(\mathbf{\Sigma})$ matrices whose (i, j) th entry is given by

$$\begin{aligned} \Omega_{k,ij} = & \sum_{p=1}^{\varrho(\mathbf{A})} \sum_{q=1}^{\ell_p(\mathbf{A})} \left\{ \mathcal{X}_{p,q}(\mathbf{A}) \sigma_{\langle k \rangle}^{n-m+i+j-1} (n-m+i+j-2)! \right. \\ & \left. \times {}_2F_0(n-m+i+j-1, q; -\xi \alpha_{\langle p \rangle} \sigma_{\langle k \rangle}) \right\} \end{aligned} \quad (173)$$

where $\mathcal{X}_{p,q}(\mathbf{A})$ is the (p, q) th characteristic coefficient of \mathbf{A} .

Proof: From the property (95) and Theorem 8, we have

$$\begin{aligned}
& \mathbb{E} \left\{ \det \left(\mathbf{I}_{m\nu} + \xi \mathbf{A} \otimes \mathbf{X} \mathbf{X}^\dagger \right)^{-1} \right\} \\
&= \mathbb{E} \left\{ \prod_{p=1}^{\varrho(\mathbf{A})} \det \left(\mathbf{I}_m + \xi \alpha_{\langle p \rangle} \mathbf{X} \mathbf{X}^\dagger \right)^{-\ell_p(\mathbf{A})} \right\} \\
&= \int \cdots \int_{0 < \lambda_m \leq \cdots \leq \lambda_1 < \infty} \prod_{k=1}^m \prod_{p=1}^{\varrho(\mathbf{A})} (1 + \xi \alpha_{\langle p \rangle} \lambda_k)^{-\ell_p(\mathbf{A})} p_{\lambda}(\lambda_1, \lambda_2, \dots, \lambda_m) d\lambda_1 d\lambda_2 \cdots d\lambda_m \\
&\stackrel{(a)}{=} \frac{1}{m! \mathcal{A}} \underbrace{\int_0^\infty \cdots \int_0^\infty}_{m\text{-fold}} \prod_{k=1}^m \left\{ \lambda_k^{n-m} \prod_{p=1}^{\varrho(\mathbf{A})} (1 + \xi \alpha_{\langle p \rangle} \lambda_k)^{-\ell_p(\mathbf{A})} \right\} \\
&\quad \times \det \left([\mathbf{G}_1 \quad \mathbf{G}_2 \quad \cdots \quad \mathbf{G}_{\varrho(\Sigma)}] \right) \det_{1 \leq i, j \leq m} (\lambda_j^{i-1}) d\lambda_1 d\lambda_2 \cdots d\lambda_m \\
&\stackrel{(b)}{=} \mathcal{A}^{-1} \det \left([\boldsymbol{\Omega}_1 \quad \boldsymbol{\Omega}_2 \quad \cdots \quad \boldsymbol{\Omega}_{\varrho(\Sigma)}] \right) \tag{174}
\end{aligned}$$

where (a) follows from the fact that the integrand is symmetric in $\lambda_1, \lambda_2, \dots, \lambda_m$ and (b) follows from the generalized Cauchy–Binet formula [29, Appendix], [30, Lemma 2], yielding the (i, j) th entry of $m \times \ell_k(\Sigma)$ matrices $\boldsymbol{\Omega}_k$, $k = 1, 2, \dots, \varrho(\Sigma)$, as

$$\Omega_{k,ij} = \int_0^\infty \prod_{p=1}^{\varrho(\mathbf{A})} (1 + \xi \alpha_{\langle p \rangle} \lambda)^{-\ell_p(\mathbf{A})} \lambda^{n-m+i+j-2} e^{-\lambda/\sigma_{\langle k \rangle}} d\lambda. \tag{175}$$

Using a partial fraction decomposition, (175) can be written as

$$\Omega_{k,ij} = \sum_{p=1}^{\varrho(\mathbf{A})} \sum_{q=1}^{\ell_p(\mathbf{A})} \mathcal{X}_{p,q}(\mathbf{A}) \int_0^\infty (1 + \xi \alpha_{\langle p \rangle} \lambda)^{-q} \lambda^{n-m+i+j-2} e^{-\lambda/\sigma_{\langle k \rangle}} d\lambda \tag{176}$$

where the characteristic coefficients $\mathcal{X}_{p,q}(\mathbf{A})$ is given by (168). We complete the proof of the theorem by evaluating the integral in (176) with the help of the following integral identity:

$$\int_0^\infty (1 + ax)^{\mu-1} x^{n-1} e^{-x/b} dx = b^n (n-1)! {}_2F_0(n, -\mu+1; -ab) \tag{177}$$

where $a, b > 0$, $n \in \mathbb{N}$, and $\mu \in \mathbb{C}$. □

Corollary 6: Let $\mathbf{X} \sim \tilde{\mathcal{N}}_{m,n}(\mathbf{0}_{m \times n}, \mathbf{\Sigma}, \mathbf{I}_n)$, $m \leq n$. Then, for $\nu \in \mathbb{N}$, we have

$$\mathbb{E} \left\{ \det(\mathbf{I}_m + \xi \mathbf{X} \mathbf{X}^\dagger)^{-\nu} \right\} = \frac{\det(\mathbf{\Omega})}{\prod_{i=1}^m (n-i)! (i-1)!} \quad (178)$$

where $\mathbf{\Omega} = (\Omega_{ij})$ is the $m \times m$ Hankel matrix whose (i, j) th entry is given by

$$\Omega_{ij} = (n - m + i + j - 2)! {}_2F_0(n - m + i + j - 1, \nu; -\xi). \quad (179)$$

Proof: It follows immediately from Theorem 10 with $\mathbf{\Sigma} = \mathbf{I}_m$, $\mathbf{A} = \mathbf{I}_\nu$, $\varrho(\mathbf{\Sigma}) = 1$, $\ell_1(\mathbf{\Sigma}) = m$, $\sigma_{\langle 1 \rangle} = 1$, $\varrho(\mathbf{A}) = 1$, $\ell_1(\mathbf{A}) = \nu$, and $\alpha_{\langle 1 \rangle} = 1$. \square

Theorem 11: Let $\mathbf{X} \sim \tilde{\mathcal{N}}_{m,n}(\mathbf{0}_{m \times n}, \mathbf{\Sigma}, \mathbf{\Psi})$, σ_i , $i = 1, 2, \dots, m$, and ψ_j , $j = 1, 2, \dots, n$, be the eigenvalues of $\mathbf{\Sigma}$ and $\mathbf{\Psi}$, respectively. Then, for $\xi \geq 0$, we have

$$\mathbb{E} \left\{ \det(\mathbf{I}_m + \xi \mathbf{X} \mathbf{X}^\dagger)^{-1} \right\} = \sum_{p=1}^{\varrho(\mathbf{\Sigma})} \sum_{q=1}^{\varrho(\mathbf{\Psi})} \sum_{i=1}^{\ell_p(\mathbf{\Sigma})} \sum_{j=1}^{\ell_q(\mathbf{\Psi})} \mathcal{X}_{p,i}(\mathbf{\Sigma}) \mathcal{X}_{q,j}(\mathbf{\Psi}) {}_2F_0(i, j; -\xi \sigma_{\langle p \rangle} \psi_{\langle q \rangle}) \quad (180)$$

where $\mathcal{X}_{p,i}(\mathbf{\Sigma})$ and $\mathcal{X}_{q,j}(\mathbf{\Psi})$ are the (p, i) th and (q, j) th characteristic coefficients of $\mathbf{\Sigma}$ and $\mathbf{\Psi}$, respectively.

Proof: It follows from Lemmas 1 and 2 that

$$\begin{aligned} \det(\mathbf{I}_m + \xi \mathbf{X} \mathbf{X}^\dagger)^{-1} &= \mathbb{E}_{\mathbf{y}_1} \left\{ \text{etr} \left(-\xi \mathbf{X}^\dagger \mathbf{y}_1 \mathbf{y}_1^\dagger \mathbf{X} \right) \right\} \\ &= \mathbb{E}_{\mathbf{y}_1, \mathbf{y}_2} \left\{ \text{etr} \left(\xi \mathbf{y}_1^\dagger \mathbf{X} \mathbf{y}_2 - \mathbf{y}_2^\dagger \mathbf{X}^\dagger \mathbf{y}_1 \right) \right\} \end{aligned} \quad (181)$$

where $\mathbf{y}_1 \sim \tilde{\mathcal{N}}_m(\mathbf{0}_m, \mathbf{I}_m)$ and $\mathbf{y}_2 \sim \tilde{\mathcal{N}}_n(\mathbf{0}_n, \mathbf{I}_n)$. Denoting the left-hand side of (180) by $\text{LHS}_{(180)}$ and using (181), we have

$$\begin{aligned} \text{LHS}_{(180)} &= \mathbb{E}_{\mathbf{y}_1, \mathbf{y}_2} \left\{ \mathbb{E}_{\mathbf{X}} \left\{ \text{etr} \left(\xi \mathbf{y}_2 \mathbf{y}_1^\dagger \mathbf{X} - \mathbf{X}^\dagger \mathbf{y}_1 \mathbf{y}_2^\dagger \right) \right\} \right\} \\ &= \mathbb{E}_{\mathbf{y}_1, \mathbf{y}_2} \left\{ \exp \left(-\xi \mathbf{y}_1^\dagger \mathbf{\Sigma} \mathbf{y}_1 \mathbf{y}_2^\dagger \mathbf{\Psi} \mathbf{y}_2 \right) \right\}. \end{aligned} \quad (182)$$

Now, introducing a delta function to decouple the expectations for \mathbf{y}_1 and \mathbf{y}_2 in (182) yields

$$\begin{aligned}
\text{LHS}_{(180)} &= \mathbb{E}_{\mathbf{y}_1, \mathbf{y}_2} \left\{ \int_{-\infty}^{\infty} e^{-\xi z \mathbf{y}_2^\dagger \mathbf{\Psi} \mathbf{y}_2} \delta(z - \mathbf{y}_1^\dagger \mathbf{\Sigma} \mathbf{y}_1) dz \right\} \\
&\stackrel{(a)}{=} \frac{1}{2\pi} \mathbb{E}_{\mathbf{y}_1, \mathbf{y}_2} \left\{ \int_{-\infty}^{\infty} \int_{-\infty}^{\infty} e^{-\xi z \mathbf{y}_2^\dagger \mathbf{\Psi} \mathbf{y}_2} e^{j(z - \mathbf{y}_1^\dagger \mathbf{\Sigma} \mathbf{y}_1)\omega} d\omega dz \right\} \\
&= \frac{1}{2\pi} \int_{-\infty}^{\infty} \int_{-\infty}^{\infty} e^{j\omega z} \mathbb{E}_{\mathbf{y}_1} \left\{ \text{etr}(-j\omega \mathbf{\Sigma} \mathbf{y}_1 \mathbf{y}_1^\dagger) \right\} \mathbb{E}_{\mathbf{y}_2} \left\{ \text{etr}(-\xi z \mathbf{\Psi} \mathbf{y}_2 \mathbf{y}_2^\dagger) \right\} d\omega dz \\
&\stackrel{(b)}{=} \frac{1}{2\pi} \int_{-\infty}^{\infty} \int_{-\infty}^{\infty} e^{j\omega z} \det(\mathbf{I}_m + j\omega \mathbf{\Sigma})^{-1} \det(\mathbf{I}_n + \xi z \mathbf{\Psi})^{-1} d\omega dz \\
&\stackrel{(c)}{=} \frac{1}{2\pi} \sum_{p=1}^{\varrho(\mathbf{\Sigma})} \sum_{q=1}^{\varrho(\mathbf{\Psi})} \sum_{i=1}^{\ell_p(\mathbf{\Sigma})} \sum_{j=1}^{\ell_q(\mathbf{\Psi})} \left\{ \mathcal{X}_{p,i}(\mathbf{\Sigma}) \mathcal{X}_{q,j}(\mathbf{\Psi}) \right. \\
&\quad \left. \times \int_{-\infty}^{\infty} \int_{-\infty}^{\infty} e^{j\omega z} (1 + j\sigma_{\langle p \rangle} \omega)^{-i} (1 + \xi \psi_{\langle q \rangle} z)^{-j} d\omega dz \right\} \quad (183)
\end{aligned}$$

where (a) is obtained by replacing the delta function with its Fourier representation, (b) follows from Lemma 1, and (c) is obtained from Definition 6. Using the integral identity, for $a > 0$, $\ell \in \mathbb{N}$, and $z \in \mathbb{R}$,

$$\int_{-\infty}^{\infty} e^{j\omega z} (1 + ja\omega)^{-\ell} d\omega = \frac{\pi z^{\ell-1} e^{-\sqrt{z^2}/a}}{a^\ell (\ell-1)!} (1 + \text{sign}(z)), \quad (184)$$

(183) can be written as

$$\text{LHS}_{(180)} = \sum_{p=1}^{\varrho(\mathbf{\Sigma})} \sum_{q=1}^{\varrho(\mathbf{\Psi})} \sum_{i=1}^{\ell_p(\mathbf{\Sigma})} \sum_{j=1}^{\ell_q(\mathbf{\Psi})} \frac{\mathcal{X}_{p,i}(\mathbf{\Sigma}) \mathcal{X}_{q,j}(\mathbf{\Psi})}{\sigma_{\langle p \rangle}^i (i-1)!} \int_0^\infty (1 + \xi \psi_{\langle q \rangle} z)^{-j} z^{i-1} e^{-z/\sigma_{\langle p \rangle}} dz. \quad (185)$$

Finally, we obtain the desired result (180) by evaluating the integral in (185) with the help of (177). \square

ACKNOWLEDGMENT

The authors would like to thank Jin Sam Kwak and Irene Keliher for their comments and careful reading of the manuscript.

REFERENCES

- [1] J. H. Winters, "On the capacity of radio communication systems with diversity in Rayleigh fading environment," *IEEE J. Select. Areas Commun.*, vol. 5, no. 5, pp. 871–878, June 1987.
- [2] G. J. Foschini, "Layered space–time architecture for wireless communication in a fading environment when using multi-element antennas," *Bell Labs Tech. J.*, vol. 1, no. 2, pp. 41–59, Autumn 1996.
- [3] G. J. Foschini and M. J. Gans, "On limits of wireless communications in a fading environment when using multiple antennas," *Wireless Personal Commun.*, vol. 6, no. 3, pp. 311–335, Mar. 1998.
- [4] Ī. E. Telatar, "Capacity of multi-antenna Gaussian channels," *European Trans. Telecommun.*, vol. 10, no. 6, pp. 585–595, Nov./Dec. 1999.
- [5] B. Wang, J. Zhang, and A. Høst-Madsen, "On the capacity of MIMO relay channels," *IEEE Trans. Inform. Theory*, vol. 51, no. 1, pp. 29–43, Jan. 2005.
- [6] V. Tarokh, N. Seshadri, and A. R. Calderbank, "Space–time codes for high data rate wireless communication: Performance criterion and code construction," *IEEE Trans. Inform. Theory*, vol. 44, no. 2, pp. 744–765, Mar. 1998.
- [7] S. M. Alamouti, "A simple transmit diversity technique for wireless communications," *IEEE J. Select. Areas Commun.*, vol. 16, no. 8, pp. 1451–1458, Oct. 1998.
- [8] V. Tarokh, H. Jafarkhani, and A. R. Calderbank, "Space–time block codes from orthogonal designs," *IEEE Trans. Inform. Theory*, vol. 45, no. 5, pp. 1456–1467, July 1999.
- [9] —, "Space–time block coding for wireless communications: Performance results," *IEEE J. Select. Areas Commun.*, vol. 17, no. 3, pp. 451–460, Mar. 1999.
- [10] S. D. Blostein and H. Leib, "Multiple antenna systems: Their role and impact in future wireless access," *IEEE Commun. Mag.*, vol. 41, no. 7, pp. 94–101, July 2003.
- [11] A. J. Paulraj, D. A. Gore, R. U. Nabar, and H. Bölcskei, "An overview of mimo communications—A key to gigabit wireless," *Proc. IEEE*, vol. 92, no. 2, pp. 198–218, Feb. 2004.
- [12] S. Parker, M. Sandell, M. S. Yee, Y. Sun, M. Ismail, P. Strauch, and J. McGeehan, "Space–time codes for future WLANs: Principles, practice, and performance," *IEEE Commun. Mag.*, vol. 42, no. 12, pp. 96–103, Dec. 2004.
- [13] O. Tirkkonen and A. Hottinen, "Square-matrix embeddable space–time block codes for complex signal constellations," *IEEE Trans. Inform. Theory*, vol. 48, no. 2, pp. 384–395, Feb. 2002.
- [14] W. Su and X.-G. Xia, "Two generalized complex orthogonal space–time block codes of rates 7/11 and 3/5 for 5 and 6 transmit antennas," *IEEE Trans. Inform. Theory*, vol. 49, no. 1, pp. 313–316, Jan. 2003.
- [15] H. Wang and X.-G. Xia, "Upper bounds of rates of complex orthogonal space–time block codes," *IEEE Trans. Inform. Theory*, vol. 49, no. 10, pp. 2788–2796, Oct. 2003.
- [16] X.-B. Liang and X.-G. Xia, "On the nonexistence of rate-one generalized complex orthogonal designs," *IEEE Trans. Inform. Theory*, vol. 49, no. 11, pp. 2984–2989, Nov. 2003.
- [17] H. Jafarkhani, "A quasi-orthogonal space–time block code," *IEEE Trans. Commun.*, vol. 49, no. 1, pp. 1–4, Jan. 2001.
- [18] B. A. Sethuraman, B. S. Rajan, and V. Shashidhar, "Full-diversity, high-rate space–time block codes from division algebras," *IEEE Trans. Inform. Theory*, vol. 49, no. 10, pp. 2596–2616, Oct. 2003.
- [19] W. Su and X.-G. Xia, "Signal constellations for quasi-orthogonal space–time block codes with full diversity," *IEEE Trans. Inform. Theory*, vol. 50, no. 10, pp. 2331–2347, Oct. 2004.
- [20] D.-S. Shiu, G. J. Foschini, M. J. Gans, and J. M. Kahn, "Fading correlation and its effect on the capacity of multielement antenna systems," *IEEE Trans. Commun.*, vol. 48, no. 3, pp. 502–513, Mar. 2000.

- [21] D. Gesbert, H. Bölcskei, D. A. Gore, and A. J. Paulraj, "Outdoor MIMO wireless channels: Models and performance prediction," *IEEE Trans. Commun.*, vol. 50, no. 12, pp. 1926–1934, Dec. 2002.
- [22] D. Chizhik, G. J. Foschini, M. J. Gans, and R. A. Valenzuela, "Keyholes, correlations, and capacities of multielement transmit and receive antennas," *IEEE Trans. Wireless Commun.*, vol. 1, no. 2, pp. 361–368, Apr. 2002.
- [23] A. F. Molisch, M. Steinbauer, M. Toeltsch, E. Bonek, and R. S. Thomä, "Capacity of MIMO systems based on measured wireless channels," *IEEE J. Select. Areas Commun.*, vol. 20, no. 3, pp. 561–569, Apr. 2002.
- [24] A. F. Molisch, "A generic model for MIMO wireless propagation channels in macro- and microcells," *IEEE Trans. Signal Processing*, vol. 52, no. 1, pp. 61–70, Jan. 2004.
- [25] C.-N. Chuah, D. N. C. Tse, J. M. Kahn, and R. A. Valenzuela, "Capacity scaling in MIMO wireless systems under correlated fading," *IEEE Trans. Inform. Theory*, vol. 48, no. 3, pp. 637–650, Mar. 2002.
- [26] S. Loyka and A. Kouki, "On MIMO channel capacity, correlations, and keyholes: Analysis of degenerate channels," *IEEE Trans. Commun.*, vol. 50, no. 12, pp. 1886–1888, Dec. 2002.
- [27] P. Almers, F. Tufvesson, and A. F. Molisch, "Measurement of keyhole effect in a wireless multiple-input multiple-output (MIMO) channel," *IEEE Commun. Lett.*, vol. 7, no. 8, pp. 373–375, Aug. 2003.
- [28] H. Shin and J. H. Lee, "Capacity of multiple-antenna fading channels: Spatial fading correlation, double scattering, and keyhole," *IEEE Trans. Inform. Theory*, vol. 49, no. 10, pp. 2636–2647, Oct. 2003.
- [29] M. Chiani, M. Z. Win, and A. Zanella, "On the capacity of spatially correlated MIMO Rayleigh-fading channels," *IEEE Trans. Inform. Theory*, vol. 49, no. 10, pp. 2363–2371, Oct. 2003.
- [30] H. Shin, M. Z. Win, J. H. Lee, and M. Chiani, "On the capacity of doubly correlated MIMO channels," *IEEE Trans. Wireless Commun.*, to be published (also available at <http://arxiv.org/abs/cs.IT/0509075>).
- [31] X. W. Cui and Z. M. Feng, "Lower capacity bound for MIMO correlated fading channels with keyhole," *IEEE Commun. Lett.*, vol. 8, no. 8, pp. 500–502, Aug. 2004.
- [32] E. A. Jorswieck and A. Sezgin, "Impact of spatial correlation on the performance of orthogonal space–time block codes," *IEEE Commun. Lett.*, vol. 8, no. 1, pp. 21–23, Jan. 2004.
- [33] J. Wang, M. K. Simon, M. P. Fitz, and K. Yao, "On the performance of space–time codes over spatially correlated Rayleigh fading channels," *IEEE Trans. Commun.*, vol. 52, no. 6, pp. 877–881, June 2004.
- [34] M. Fozunbal, S. W. McLaughlin, R. W. Schafer, and J. M. Landsberg, "On space–time coding in the presence of spatial-temporal correlation," *IEEE Trans. Inform. Theory*, vol. 50, no. 9, pp. 1910–1926, Sept. 2004.
- [35] R. U. Nabar, H. Bölcskei, and A. J. Paulraj, "Diversity and outage performance in space–time block coded Ricean MIMO channels," *IEEE Trans. Wireless Commun.*, 2005, to be published.
- [36] A. Maaref and S. Aïssa, "Exact capacity and symbol-error probability analysis for STBC in spatially correlated MIMO Nakagami fading channels," in *Proc. IEEE Global Telecommun. Conf. (Globecom'05)*, St. Louis, MO, Nov. 2005.
- [37] —, "Capacity of space–time block codes in MIMO Rayleigh fading channels with adaptive transmission and estimation errors," *IEEE Trans. Wireless Commun.*, vol. 4, no. 5, Sept. 2005.
- [38] H. Shin and J. H. Lee, "Effect of keyholes on the symbol error rate of space–time block codes," *IEEE Commun. Lett.*, vol. 7, no. 1, pp. 27–29, Jan. 2003.
- [39] —, "Performance analysis of space–time block codes over keyhole Nakagami- m fading channels," *IEEE Trans. Veh. Technol.*, vol. 53, no. 2, pp. 351–362, Mar. 2004.
- [40] A. M. N. Nasrabadi, H. R. Bahrami, and S. H. Jamali, "Space–time trellis codes for keyhole channels: Performance criterion and code design," *Electron. Lett.*, vol. 40, no. 1, pp. 53–55, Jan. 2004.

- [41] S. Sanayei, A. Hedayat, and A. Nosratinia, "Space-time codes in keyhole channels: Analysis and design," in *Proc. IEEE Global Communications Conf. (GLOBECOM'04)*, Dallas, TX, Nov. 2004, pp. 3768–3772.
- [42] M. Z. Win and J. H. Winters, "Analysis of hybrid selection/maximal-ratio combining in Rayleigh fading," *IEEE Trans. Commun.*, vol. 47, no. 12, pp. 1773–1776, Dec. 1999.
- [43] M. Z. Win and Z. A. Kostić, "Impact of spreading bandwidth on rake reception in dense multipath channels," vol. 17, no. 10, Oct. 1999.
- [44] M. Z. Win, "Distribution-invariant monotonicity theorems on multi-channel diversity," *IEEE Trans. Wireless Commun.*, 2005, to be published.
- [45] S. Verdú, "Spectral efficiency in the wideband regime," *IEEE Trans. Inform. Theory*, vol. 48, no. 6, pp. 1319–1343, June 2002.
- [46] A. Lozano, A. M. Tulino, and S. Verdú, "Multiple-antenna capacity in the low-power regime," *IEEE Trans. Inform. Theory*, vol. 49, no. 10, pp. 2527–2544, Oct. 2003.
- [47] M. K. Simon, S. M. Hindei, and W. C. Lindsey, *Digital Communication Techniques: Signal Design and Detection*. Englewood Cliffs, NJ: Prentice Hall, 1995.
- [48] M. K. Simon and M.-S. Alouini, *Digital Communication over Fading Channels: A Unified Approach to Performance Analysis*. New York: Wiley, 2000.
- [49] M. Chiani, M. Z. Win, and A. Zanella, "Error probability for optimum combining of M -ary PSK signals in the presence of interference and noise," *IEEE Trans. Commun.*, vol. 51, no. 11, pp. 1949–1957, Nov. 2003.
- [50] —, "On optimum combining of M -PSK signals with unequal-power interferers and noise," *IEEE Trans. Commun.*, vol. 53, no. 1, pp. 44–47, Jan. 2005.
- [51] K. Pearson, "Das Fehlergesetz und Seine Verallgemeinerungen Durch Fechner und Pearson. A Rejoinder," *Biometrika*, vol. 4, no. 1/2, pp. 169–212, June 1905.
- [52] S. Shamai (Shitz) and S. Verdú, "The impact of frequency-flat fading on the spectral efficiency of CDMA," *IEEE Trans. Inform. Theory*, vol. 47, no. 4, pp. 1302–1327, May 2001.
- [53] U. Charash, "Reception through Nakagami fading multipath channels with random delays," *IEEE Trans. Commun.*, vol. 27, no. 4, pp. 657–670, Apr. 1979.
- [54] X. Dong, N. C. Beaulieu, and P. H. Wittke, "Error probabilities of two-dimensional M -ary signaling in fading," *IEEE Trans. Commun.*, vol. 47, no. 3, pp. 352–355, Mar. 1999.
- [55] I. Schur, "Über eine Klasse von Mittelbildungen mit Anwendungen auf die Determinantentheorie," *Sitzungsbericht der Berliner Mathematischen Gesellschaft*, vol. 22, pp. 9–20, 1923.
- [56] L. A. Shepp, "Private conversation," Nov. 1999, AT&T Laboratories.
- [57] T. Ando, "Majorizations, doubly stochastic matrices, and comparison of eigenvalues," *Linear Algebra Appl.*, vol. 118, pp. 163–248, June 1989.
- [58] R. A. Horn and C. R. Johnson, *Topics in Matrix Analysis*. Cambridge, U.K.: Cambridge Univ. Press, 1991.
- [59] R. B. Bapat and V. S. Sunder, "On majorization and Schur products," *Linear Algebra Appl.*, vol. 72, pp. 107–117, Dec. 1985.
- [60] S. A. Jafar and A. Goldsmith, "Multiple-antenna capacity in correlated Rayleigh fading with channel covariance information," *IEEE Trans. Wireless Commun.*, vol. 4, no. 3, pp. 990–997, May 2005.
- [61] J. N. Pierce and S. Stein, "Multiple diversity with nonindependent fading," *Proc. IRE*, vol. 48, pp. 89–104, Jan. 1960.

- [62] V. A. Aalo, "Performance of maximal-ratio diversity systems in a correlated Nakagami-fading environment," *IEEE Trans. Commun.*, vol. 43, no. 8, pp. 2360–2369, Aug. 1995.
- [63] M.-S. Alouini, A. Abdi, and M. Kaveh, "Sum of Gamma variates and performance of wireless communication systems over Nakagami-fading channels," *IEEE Trans. Veh. Technol.*, vol. 50, no. 6, pp. 1471–1480, Nov. 2001.
- [64] A. K. Gupta and D. K. Nagar, *Matrix Variate Distributions*. Boca Raton, FL: Chapman & Hall/CRC, 2000.
- [65] A. T. James, "The distribution of the latent roots of the covariance matrix," *Ann. Math. Statistics*, vol. 31, no. 1, pp. 151–158, Mar. 1960.
- [66] —, "Distributions of matrix variates and latent roots derived from normal samples," *Ann. Math. Statistics*, vol. 35, no. 2, pp. 475–501, June 1964.
- [67] C. G. Khatri, "On certain distribution problems based on positive definite quadratic functions in normal vectors," *Ann. Math. Statistics*, vol. 37, no. 2, pp. 468–479, Apr. 1966.
- [68] —, "On the moments of traces of two matrices in three situations for complex multivariate normal populations," *Sankhya, The Indian J. Statistics, Series A*, vol. 32, pp. 65–80, Mar. 1970.
- [69] A. Takemura, *Zonal Polynomials*. Hayward, CA: Institute of Mathematical Statistics Lecture Note–Monograph Series, Vol. 4, 1984.
- [70] I. S. Gradshteyn and I. M. Ryzhik, *Table of Integrals, Series, and Products*, 6th ed. San Diego, CA: Academic, 2000.
- [71] I. G. Macdonald, *Symmetric Functions and Hall Polynomials*, 2nd ed. New York: Oxford University Press, 1999.
- [72] A. P. Prudnikov, Y. A. Brychkov, and O. I. Marichev, *Integrals and Series*. New York: Gordon and Breach Science, 1990, vol. 3.
- [73] G. L. Turin, "The characteristic function of Hermitian quadratic forms in complex normal variables," *Biometrika*, vol. 47, pp. 199–201, June 1960.
- [74] M. Evans, N. Hastings, and B. Peacock, *Statistical Distributions*, 3rd ed. New York: Wiley, 2000.
- [75] J. G. Christiano and J. E. Hall, "On the n -th derivative of a determinant of the j -th order," *Mathematics Magazine*, vol. 37, no. 4, pp. 215–217, Sept. 1964.

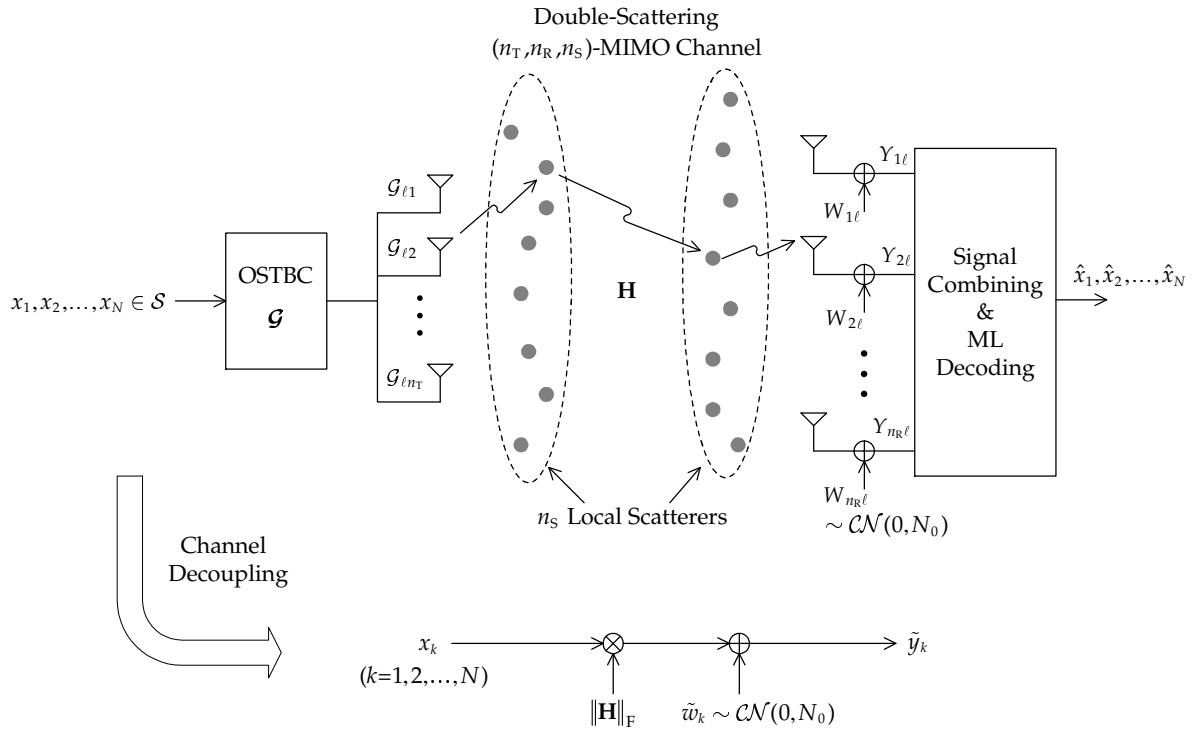


Fig. 1. Block diagram of a space-time block coded system in double-scattering (n_T, n_R, n_S) -MIMO channels and induced SISO subchannels.

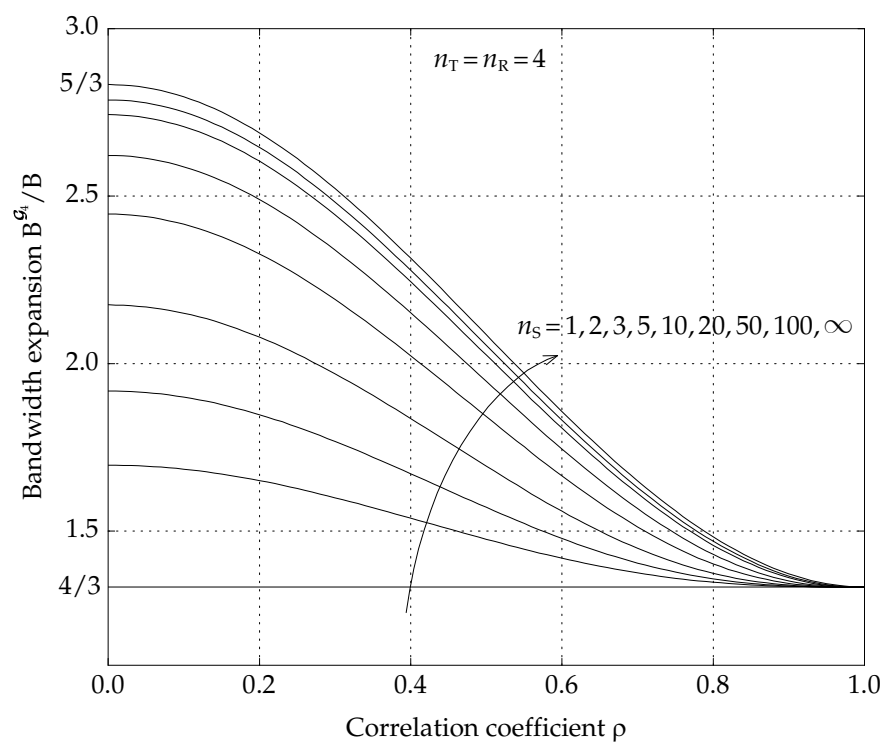


Fig. 2. Variation of the bandwidth expansion $\frac{B^{G_4}}{B}$ with a correlation coefficient ρ in double-scattering $(4, 4, n_S)$ -MIMO channels with exponential correlation $\Phi_T = \Phi_R = \Phi_4^{(e)}(\rho)$ and $\Phi_S = \Phi_{n_S}^{(e)}(\rho)$. $n_S = 1, 2, 3, 5, 10, 20, 50, 100$, and ∞ .

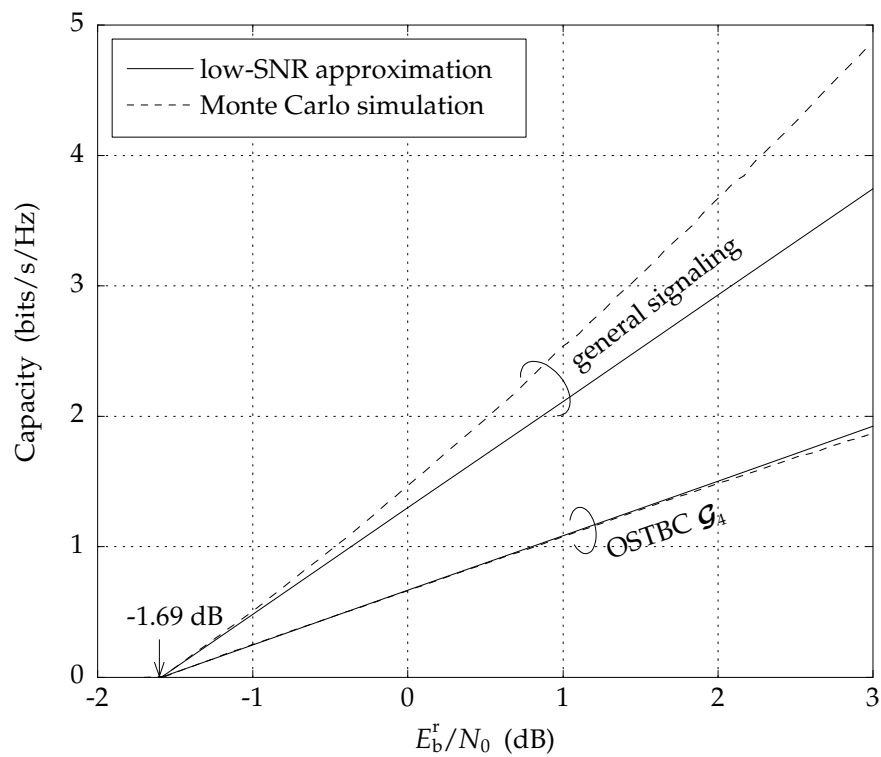


Fig. 3. Capacity in bits/s/Hz versus the received $\frac{E_b}{N_0}$ for the general input signaling and OSTBC \mathcal{G}_4 in double-scattering $(4, 4, 20)$ -MIMO channels with exponential correlation $\Phi_T = \Phi_R = \Phi_4^{(e)}(0.5)$ and $\Phi_S = \Phi_{20}^{(e)}(0.5)$.

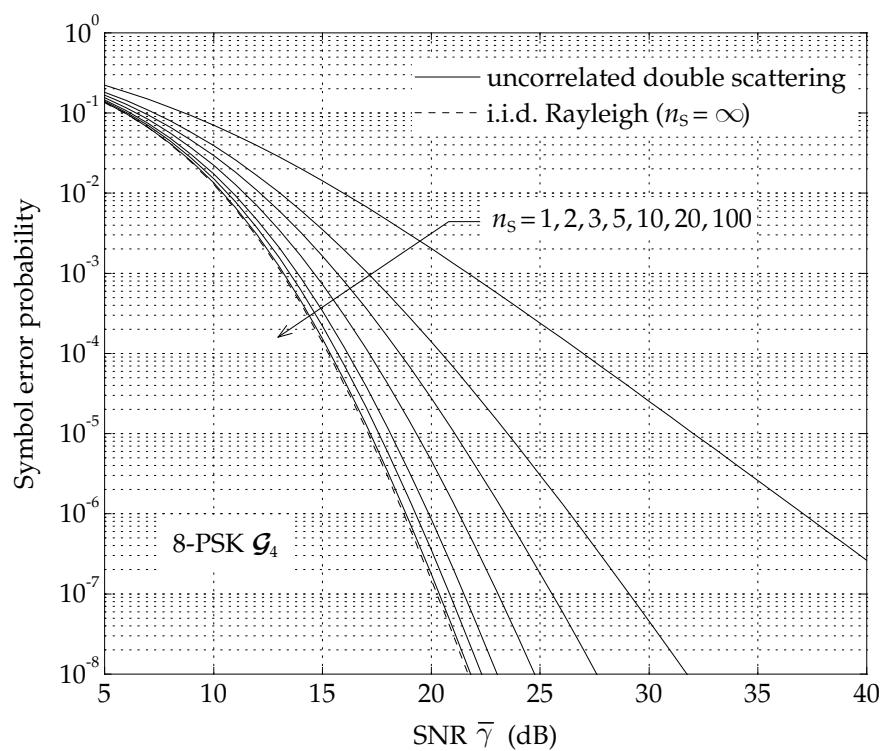


Fig. 4. SEP of 8-PSK \mathcal{G}_4 (2.25 bits/s/Hz) versus $\bar{\gamma}$ in spatially uncorrelated double-scattering $(4, 2, n_s)$ -MIMO channels. $n_s = 1, 2, 3, 5, 10, 20, 50, 100, \infty$ (i.i.d. Rayleigh).

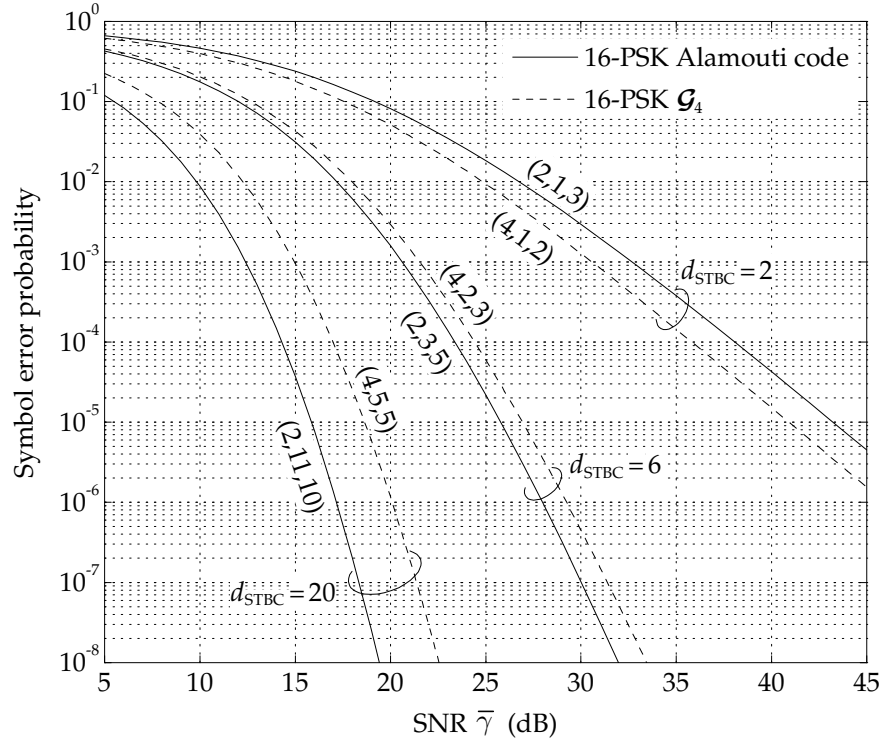


Fig. 5. SEP of 16-PSK Alamouti (4 bits/s/Hz) and \mathcal{G}_4 (3 bits/s/Hz) OSTBCs versus $\bar{\gamma}$ in spatially uncorrelated double-scattering (n_T, n_R, n_S) -MIMO channels. The Alamouti and \mathcal{G}_4 codes achieve the diversity order of $d_{\text{STBC}} = 2$ in $(2, 1, 3)$ and $(4, 1, 2)$ links, respectively. The d_{STBC} 's for $(2, 3, 5)$, $(4, 2, 3)$ and $(2, 11, 10)$, $(4, 5, 5)$ pairs are 6 and 20, respectively.

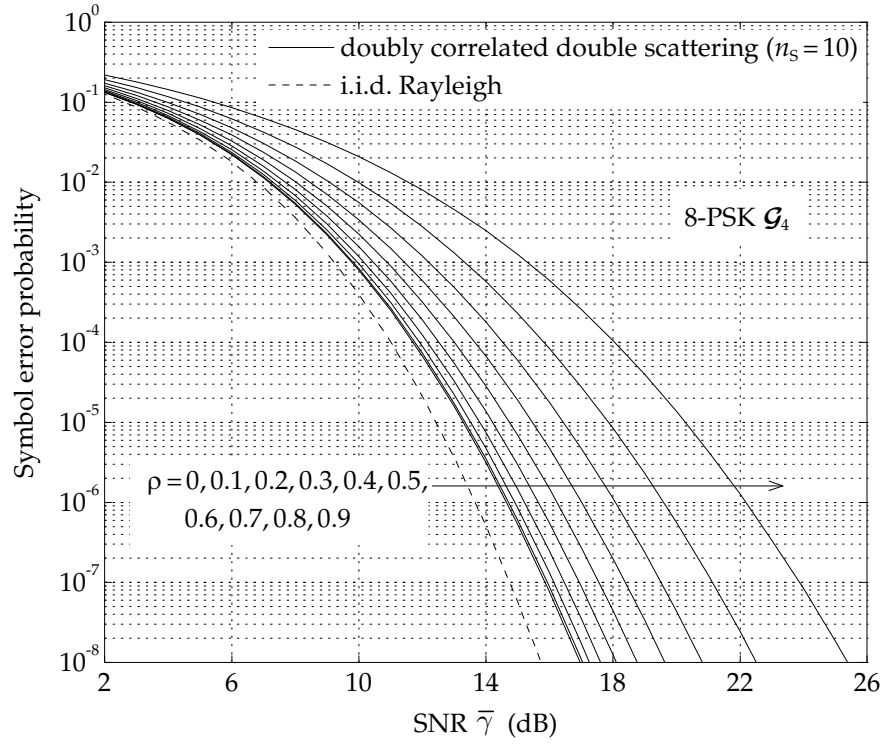


Fig. 6. SEP of 8-PSK \mathcal{G}_4 (2.25 bits/s/Hz) versus $\bar{\gamma}$ in doubly correlated double-scattering (4, 4, 10)-MIMO channels. The transmit and receive correlations follow the constant correlation $\Phi_T = \Phi_R = \Phi_4^{(c)}(\rho)$ for $\rho = 0$ (spatially uncorrelated double-scattering), 0.1, 0.2, 0.3, 0.4, 0.5, 0.6, 0.7, 0.8, and 0.9. For comparison, the SEP for i.i.d. Rayleigh-fading MIMO channels is also plotted.

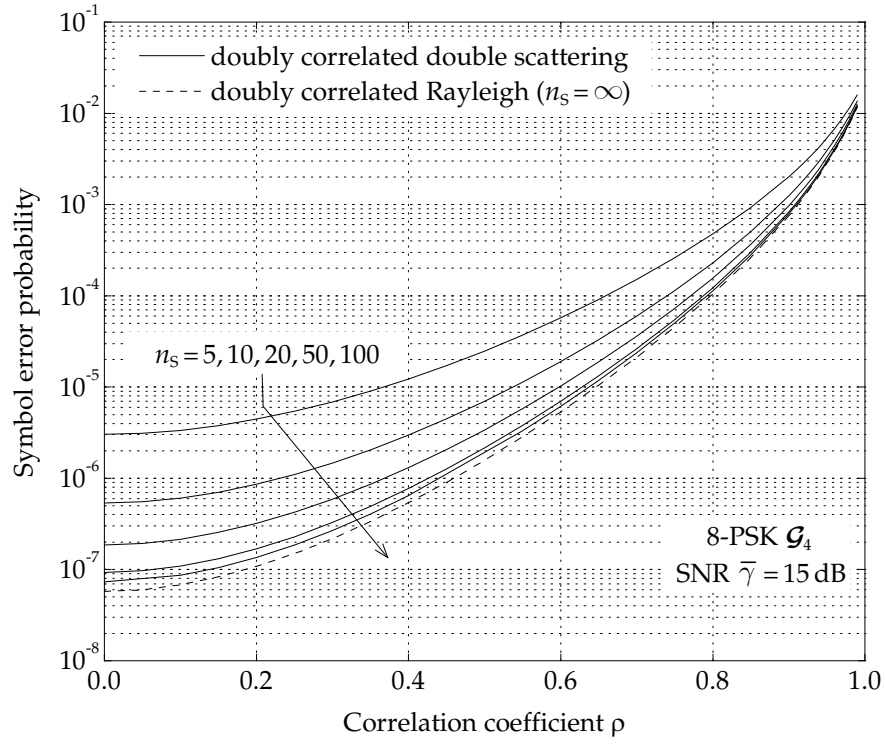


Fig. 7. SEP of 8-PSK \mathcal{G}_4 (2.25 bits/s/Hz) as a function of correlation coefficient ρ in doubly correlated double-scattering $(4, 4, n_S)$ -MIMO channels with constant correlation $\Phi_T = \Phi_R = \Phi_4^{(c)}(\rho)$. $n_S = 5, 10, 20, 50, 100, \infty$ (doubly correlated Rayleigh) and $\bar{\gamma} = 15$ dB.

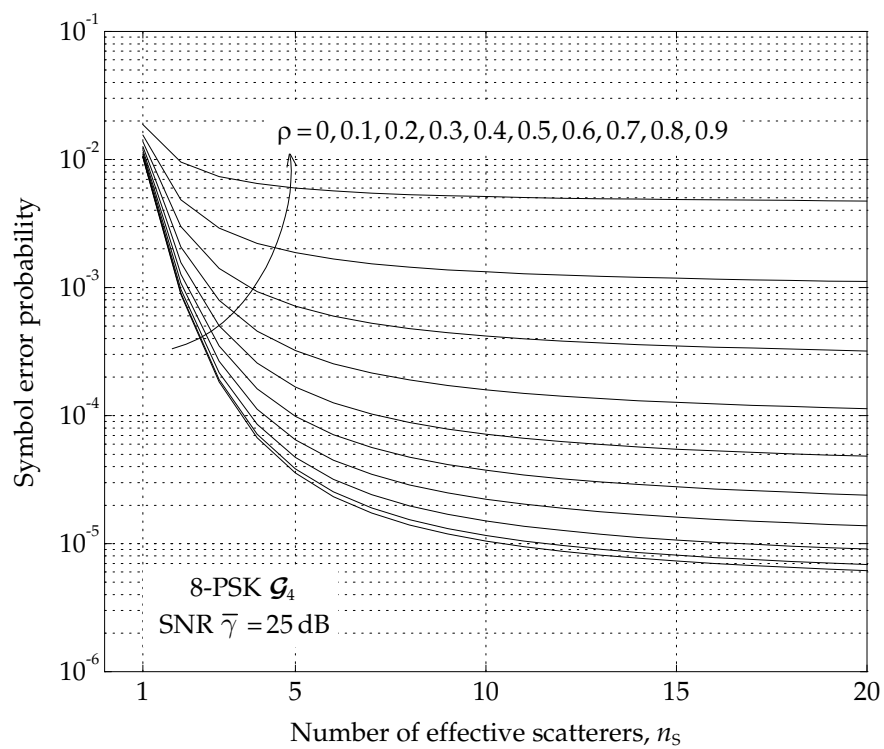


Fig. 8. SEP of 8-PSK \mathcal{G}_4 (2.25 bits/s/Hz) versus n_s in double-scattering $(4, 1, n_s)$ -MIMO channels. The transmit and scatterer correlations follow the constant correlation $\Phi_T = \Phi_4^{(c)}(\rho)$ and $\Phi_S = \Phi_{n_s}^{(c)}(\rho)$ for $\rho = 0, 0.1, 0.2, 0.3, 0.4, 0.5, 0.6, 0.7, 0.8$, and 0.9 . $\bar{\gamma} = 25$ dB.